The Strength of Metals under Combined Alternating Bending and Torsion with Phase Difference.

By

Toshio Nishihara and Minoru Kawamoto.

Abstract.

A new fatigue testing machine capable of making experiments under combined alternating bending and torsion with any phase difference has been devised and proved to be satisfactory in operation by the authors. From the test results obtained by experiments carried out on some metals with the machine, the effect of phase difference on the strength of the metals under combined bending and torsion has been made clear.

I. Introduction.

Inquiring into various practical cases in which machine parts have failed by fatigue, it is ascertained that fatigue failure of many important machine parts are caused under combined stress conditions. Among the many cases of combined stress, the case of the combination of bending and torsion is most usually encountered in practice. It is therefore an important matter to investigate the fatigue resistance of various metals under combined alternating bending and torsion.

The authors have previously carried out experiments on the strength of metals under combined alternating bending and torsion[1]. In those exments both waves of bending and torsional stresses were in phase; i.e., those stresses reached their maximum and minimum values simultaneously. However, in many cases of engineering practice, e. g. in crank-shaft, the bending and torsional stresses are not in phase, and so it is incorrect to apply the data obtained from the fatigue tests under combined stresses in phase to the practical design of such cases. We must study the effect of phase difference upon the fatigue resistance of metals.

As far as the authors are aware, no fatigue tests have yet been carried out under the combined stress conditions with phase differences. A description has, however, been published of a machine, installed in the Applied Mechanics Department of the University of Göttingen, which will be capable of carrying out the fatigue tests under combined direct and shearing stress with phase differences[2]. But no test results carried out with the machine under the combined stress conditions with phase differences have been reported.

In the authors' previous experiments mentioned above on the fatigue resistance of metals under combined alternating bending and torsional stresses in phase, the fatigue testing machine used was that specially designed by them. But in that machine the combined bending and torsional stresses were necessarily in phase, because of its mode of construction. Now the authors have recently devised a new machine for testing the combined stress fatigue. It is applicable for making experiments under combined bending and torsional stresses with an arbitrary phase difference and is found satisfactory both in construction and operation.

Experiments were made with the new testing machine on the four metals: hard steel, mild steel, cast iron, and duralumin. From the test results, the effect of phase differences on the strength of those metals under combined alternating bending and torsion was made clear experimentally. On the other hand, the authors have recently published a paper on a new criterion for the strength of metals under combined alternating stresses; in the paper the case was discussed in which both direct and shear stresses alternate between two equal magnitudes of mutually opposite signs and are not in phase, that is quite similar to the case in the present paper. By comparing the criterion proposed in the previous paper with the results of the experiments obtained here, it is proved to be satisfactory in application.

II. Description of the New Fatigue Testing Machine.

(1) *General construction of the machine.*

The new fatigue testing machine employed for the present tests was specially designed by the authors. Its principle is somewhat analogous to the other fatigue testing machines of the Nishihara type. The specimen is subjected to repeated stresses by the inertia force of the fly wheel oscillated by crank and eccentric mechanisms. In the machine

(1) T. Nishihara and M. Kawamoto, "The Strength of Metals under Combined Alternating Bending and Torsion," Memoirs of the College of Engineering, Kyoto Imperial University, Vol. X, No. 6 (1941), p. 117.

(2) E. Lehr and W. Prager, "Dauerprüfmaschine für überlagerte Zug-Druck-und-Schub-Wechselbeanspruchung," Forschung auf dem Gebiete des Ingenieurwesens, Vol. 4 (1933), Ausgabe A, p. 209.

previously reported by the authors,[3] for testing combined bending and torsional fatigue, a phase difference could not be given on the applied bending and torsional stresses, due to the fact that the fly wheel exerting both bending and torsional stresses on the specimen was oscillated by only a single crank and eccentric mechanism. With the new testing machine the fly wheel is designed to be oscillated by the different crank and eccentric mechanisms for bending and torsion respectively.

Fig. 1 (a) and 1 (b) are the explanative skeletons of the principle of the new fatigue testing machine. The former shows the plan and the latter the general arrangement. The fly wheel F is supported with ball bearings B_1 and B_2, so that it can be rotated about xx-axis and yy-axis simultaneously. The test piece T is attached between the fly wheel F and the arm A with a key and a cotter. The shaft S which rotates the eccentric disc E_1 is driven by a belt from a motor at a constant speed. The

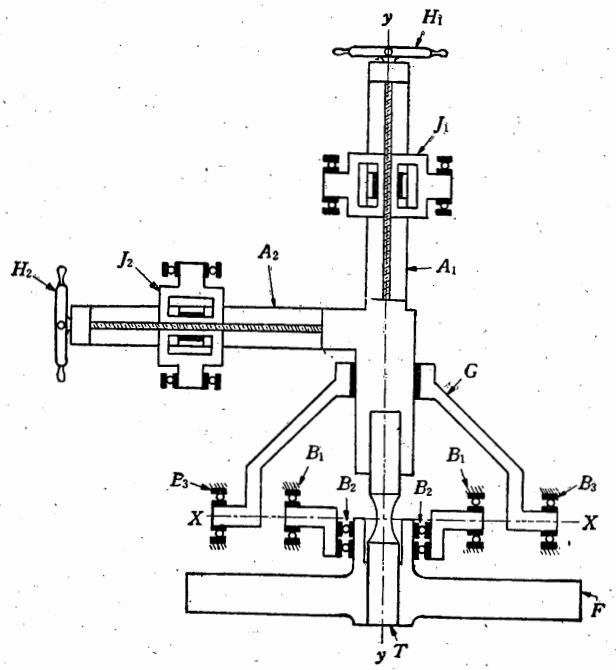

Fig. 1 (a).
Explanative Plan of the New Combined Stress Fatigue Testing Machine.

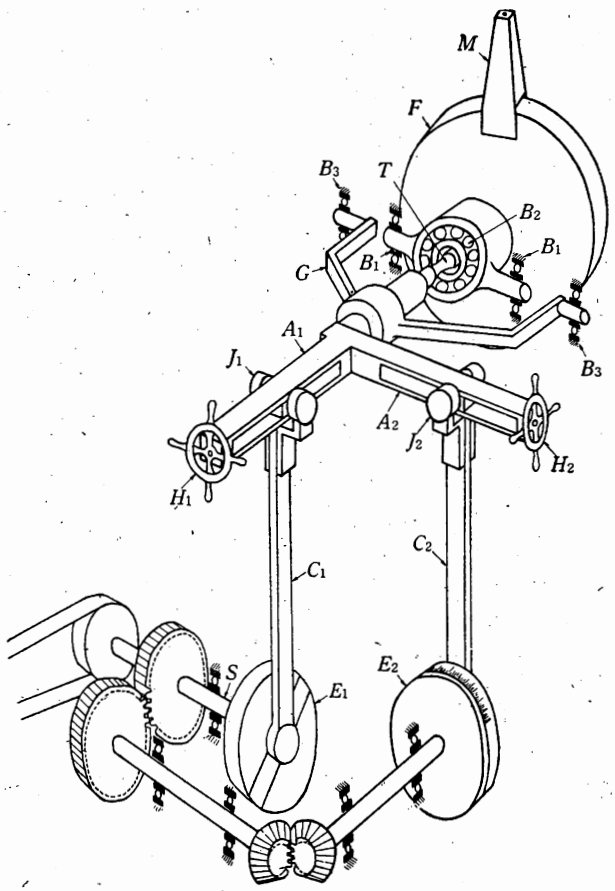

Fig. 1 (b).
General Arrangement of the New Combined Stress Fatigue Testing Machine.

arm A_1 is connected with the eccentric disc E_1 by the connecting rod C_1, so that it is oscillated in a vertical plane about the xx-axis by the action of the disc E_1 and the rod C_1. The oscillation is transmitted to the fly wheel F through the test piece T, and the fly wheel F is oscillated in a vertical plane about the center axis of the ball bearings B_1B_1 or xx-axis. Then the inertia force of the fly wheel due to the lateral oscillation exerts bending moment on the test piece. On the other hand, the eccentric disc E_2 is driven by the shaft S through the two pairs of spur gears and bevel gears. The arm A_2 is connected with the eccentric disc E_2 through the connecting rod C_2, and it is oscillated in a vertical plane about yy-axis by the action of the disc E_2 and the rod C_2. The oscillation is transmitted to the fly wheel F through the test piece T, and the fly wheel is oscillated in the circumferential direction about the center axis of the ball bearings B_2B_2, so that the inertia force of the fly wheel due to the rotary oscillation exerts torsional moment on the test piece.

The eccentric disc E_2 is composed of two discs. The one is clamped to the rotating shaft with a key and is attached to the other with two bolts. On the lateral surface of the former disc there is marked a scale of degrees, so that the latter disc can be attached to the former at any desired degree of the scale. If the scale is adjusted to zero degree, the bending and torsional stresses come in phase. The phase difference between bending and torsion can be made to come to any desired value by adjusting the angle of the scale. The junction J_1,

(3) See foot-note (1).

which connect the arm A_1 and the connecting rod C_1, is composed of two bearings perpendicular to each other similar to a universal joint. The junction J_2 has also the same construction so that there occurs no trouble at the junctions J_1 and J_2, even when the both eccentric discs are driven simultaneously.

The positions of the junctions J_1 and J_2 can be shifted by operating the handles H_1 and H_2, so that the effective lengths of the arms A_1 and A_2 can be adjusted. This adjusting can be made while the machine is working so that a fine adjustment of the amplitude of the oscillation of the fly wheel F can be made without stopping the machine. The lever G is supported with the two ball bearings B_3B_3, the center axes of which are on xx-axis. This lever guides the arm A_1 or A_2 as to be oscillated accurately with xx-axis as a center, so that the test piece T is not subjected to shearing stress.

Fig. 2 shows the assembly drawing of the new machine for testing the combined stress fatigue and Fig. 3 is its exterior view.

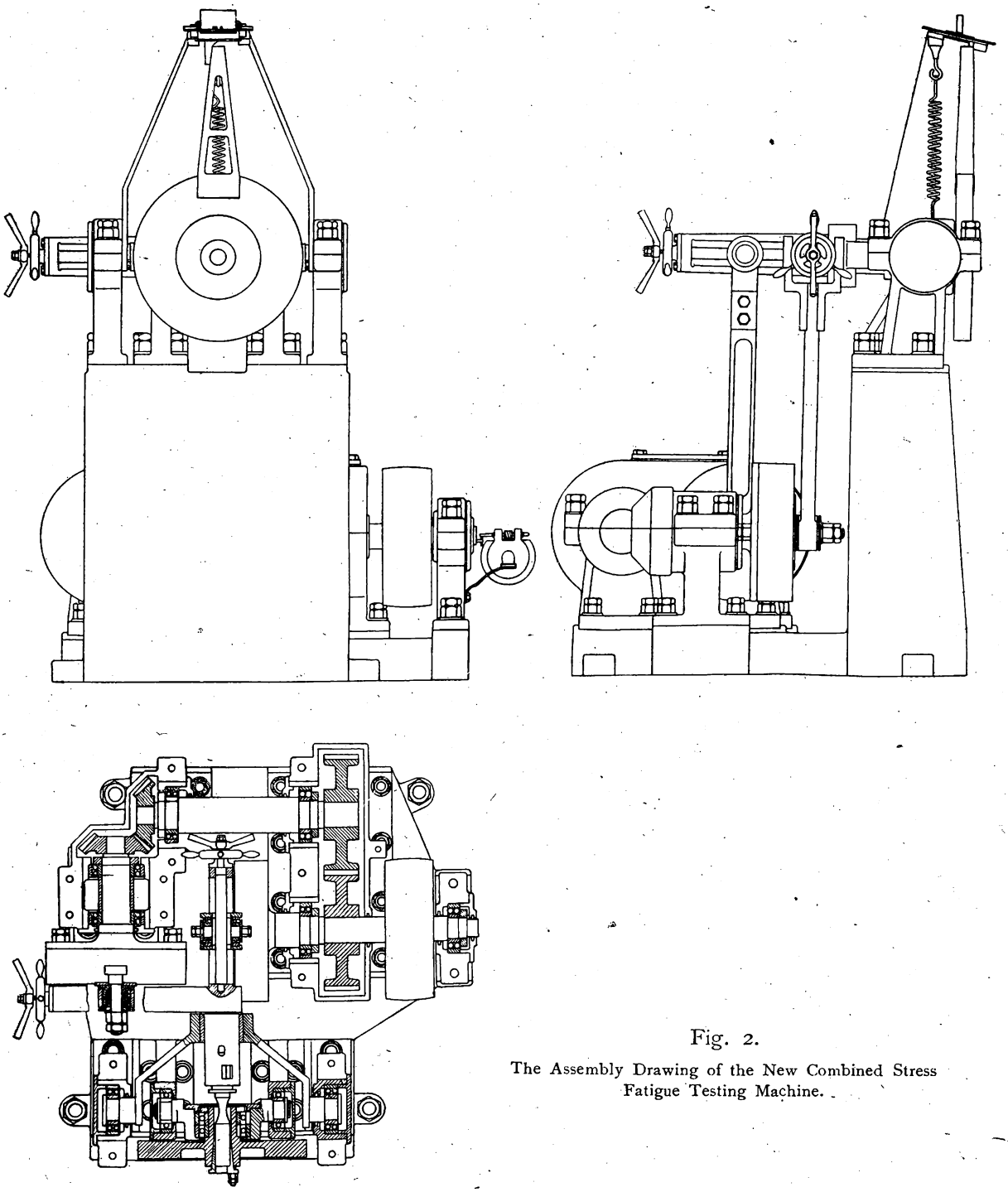

Fig. 2.

The Assembly Drawing of the New Combined Stress Fatigue Testing Machine.

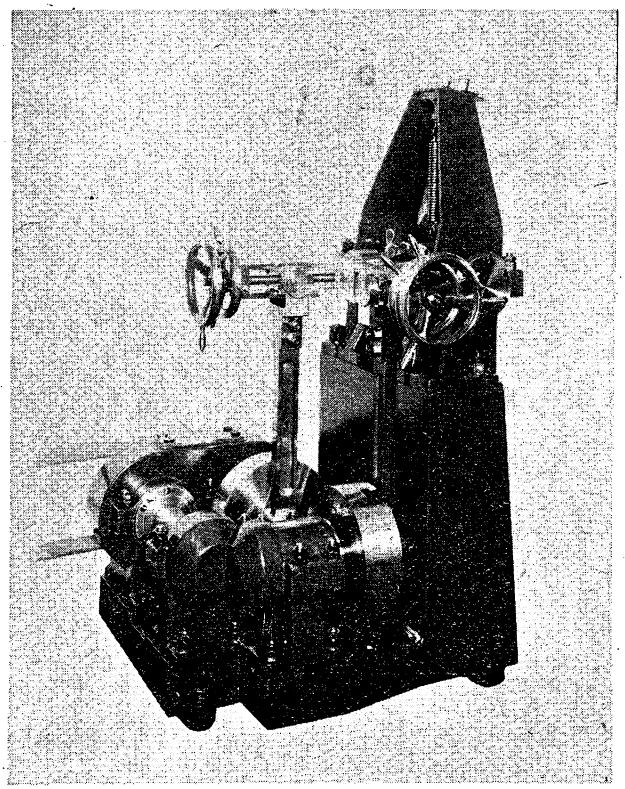

Fig. 3.
Exterior View of the New Combined Stress Fatigue Testing Machine.

(2) *Maximum stresses applied to the test piece.*

The maximum bending and torsional stresses applied to the test piece can be calculated from measurements of the amplitude and frequency of oscillation of the fly wheel, for the moments of inertia of the fly wheel about xx- and yy-axes are previously obtained by calculation. Let

I_b=moment of inertia of the fly wheel about xx-axis in kg · cm · s^2.
I_t=moment of inertia of the fly wheel about yy-axis in kg · cm · s^2.
α_b=amplitude of oscillation of the fly wheel about xx-axis in radian.
α_t=amplitude of oscillation of the fly wheel about yy-axis in radian.
M_b=maximum bending moment applied to the test piece in kg · cm.
M_t=maximum torsional moment applied to the test piece in kg · cm.
σ_a=maximum bending stress applied to the test piece in kg/cm^2.
τ_a=maximum torsional stress applied to the test piece in kg/cm^2.
d=diameter of the test piece in cm.
n=number of oscillations per minute.

Then

$$\left.\begin{aligned} M_b &= \frac{\pi d^3}{32}\sigma_a = I_b\alpha_b\left(\frac{\pi n}{30}\right)^2 \\ M_t &= \frac{\pi d^3}{16}\tau_a = I_t\alpha_t\left(\frac{\pi n}{30}\right)^2 \end{aligned}\right\} \quad (1)$$

In the design of the testing machine, the moment of inertia of the fly wheel about xx-axis was planned to be made equal to that about yy-axis:

$$I_b = I_t$$

Therefore, as is known from equation (1), bending moment M_b becomes equal to torsional moment M_t, when the amplitude α_b about xx-axis is equal to the amplitude α_t about yy-axis. In other words, the maximum moment applied to the test piece is proportional to the amplitude of the fly wheel, whether it be bending or torsion. However, if it is intended to make the maximum stress applied to the test piece proportional to the amplitude of the fly wheel, the moment of inertia of the fly wheel about xx-axis should be made equal to twice that about yy-axis, that is

$$2I_b = I_t$$

After the machine was constructed, the dimension of each part was measured accurately, and the moment of inertia of the fly wheel was calculated over again. It was found that there was a small difference between the two moments of inertia as follows:

$$I_b = 0.6364 \text{ kg} \cdot \text{cm} \cdot \text{s}^2$$
$$I_t = 0.6578 \text{ kg} \cdot \text{cm} \cdot \text{s}^2$$

(3) *The device for measuring the applied stress.*

To measure the amplitude of oscillation of the fly wheel, the arm M is attached to it. At the tip of the arm, there is a small hole of 1 mm diameter, and the interior is illuminated with a small lamp, so that by looking downwards, we can observe the small hole as a bright spot. When the alternating bending stress is applied to the test piece, the spot vibrates in the vertical direction, and when the alternating torsional stress is applied, it vibrates in the horizontal direction. Hence, when the combined bending and torsional stresses are applied to the test piece, the spot vibrates in the horizontal and vertical direction simultaneously, making the bright spot describe generally an ellipse.

Fig. 4 shows the loci of the bright spot in various combined stress conditions photographed by an ordinary camera. Value of θ in Fig. 4 is represented by the following expression:

$$\tan\theta = \frac{M_b}{M_t}$$

Hence, when θ is 0 degree, it corresponds to the

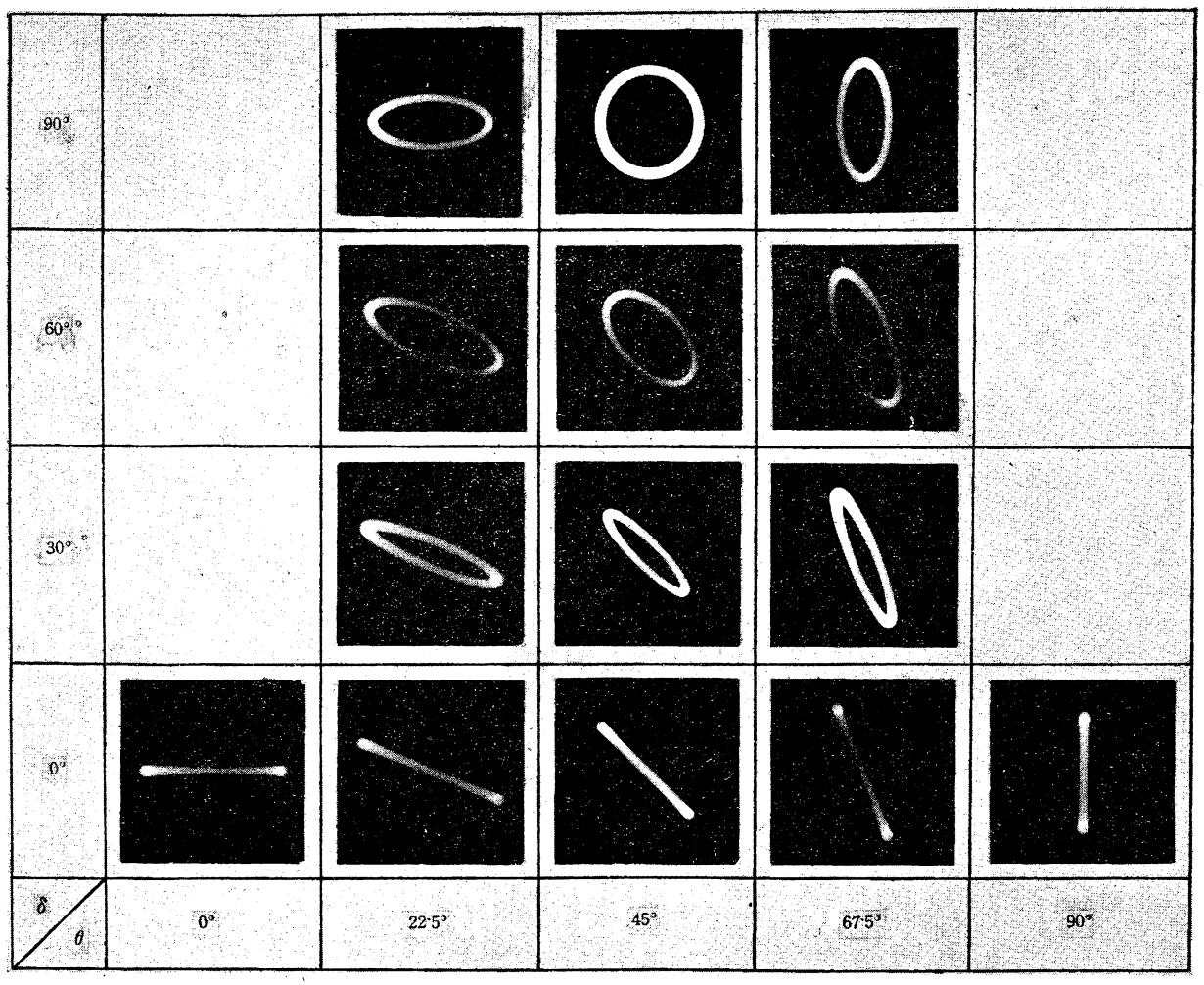

$\tan\theta=\frac{M_b}{M_t}$, δ=Phase Difference

Fig. 4.

Loci of the Bright Spot. (Time of Exposure=30 s., Driving Speed of the Testing Machine=1140 rev/mn.)

case in which only the torsional stress is working, and when θ is 90 degrees, it corresponds to the case, in which only the bending stress is working. These relations are quite analogous to the relations given in a previous report[4]. Also in Fig. 2

δ=angle of phase difference between bending and torsion.

When δ is 0 degree, i. e. bending and torsional stresses are in phase, the locus becomes a straight line, and when δ is not 0 degree, the locus becomes generally an ellipse. And the eccentricity of the ellipse becomes smaller, as δ increases. When δ is 90 degrees, the principal axes of the ellipse become perpendicular to each other, and when θ is 45 degrees and δ is 90 degrees, the ellipse becomes nearly a circle.

By measuring these ellipses or straigt lines, we can calculate the bending and torsional stresses applied to the test piece. The curve $A\ B\ C\ D$ in Fig. 5 is regarded as the outer boundary of the ellipse drawn by the bright spot. Let the tangent

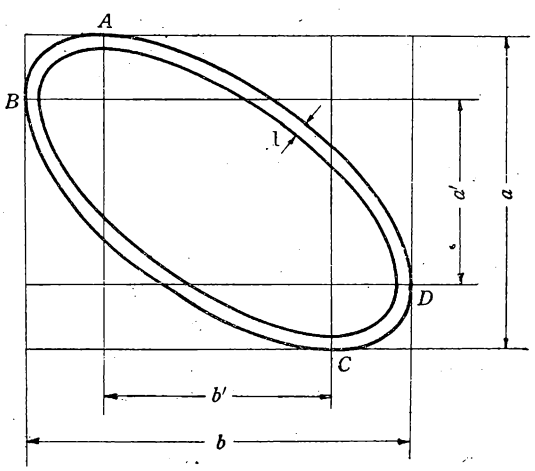

Fig. 5.

A Locus of the Bright Spot.

(4) See foot-note (1).

points of this outer boundary with horizontal and vertical straight lines be A, B, C and D as shown in Fig. 5. Also let

a=distance between A and C measured in the vertical direction, mm.

b=distance between B and D measured in the horizontal direction, mm.

a'=distance between B and D measured in the vertical direction, mm.

b'=distance between A and C measured in the horizontal direction, mm.

r_b=distance between the tip of the arm and xx-axis, mm.

r_t=distance between the tip of the arm and yy-axis, mm.

then the amplitudes of the fly wheel a_b and a_t and phase difference δ are represented by the following relations, because the locus of the bright spot is 1 mm in width:

$$\left.\begin{aligned} a_b &= \frac{a-1}{2r_b}, \\ a_t &= \frac{b-1}{2r_t}, \end{aligned}\right\} \quad (2)$$

$$\cos\delta = \frac{a'}{a-1} = \frac{b'}{b-1}, \quad (3)$$

where r_b and r_t are the definite values for the testing machine, that is,

$$r_b = 315 \text{ mm}, \quad r_t = 310 \text{ mm}.$$

Therefore, if we obtain the values of a, b, a', and b' by measurements, we can calculate the bending and torsional stresses applied to the test piece and also the phase difference from equations (1), (2) and (3). To calculate the phase difference, there is no need of measuring both the values of a' and b'; it is sufficient to measure either one in practice.

To measure the values of a, b, a' and b', a measuring plate is attached to the frame of the testing machine just above the tip of the arm M. Fig. 6 shows the measuring plate. There is on it a sliding plate P which can be slid both in horizontal and vertical directions. The sliding amount of the plate P in the vertical direction can be measured by the scale L, and that in the horizontal direction by the scale K. The plate has a vertical and a horizontal slit. By the vertical slit we can measure the sliding amount of the plate P in the horizontal direction, and by the horizontal slit we can measure that in the vertical direction. a, b, a' and b' can be thus measured. In measuring a' and b', the tangent points must be found between the ellipse and the edge of the slit. Before the machine was constructed, some anxiety was entertained about the posibility of an accurate measurement of the tangent points. In practice, however, it is found that an accurate and satisfactory measurement of the tangent points can be made: the error in the measurement is scarcely greater than 0.1 mm, while values of a and b are ordinarily about 10~20 mm.

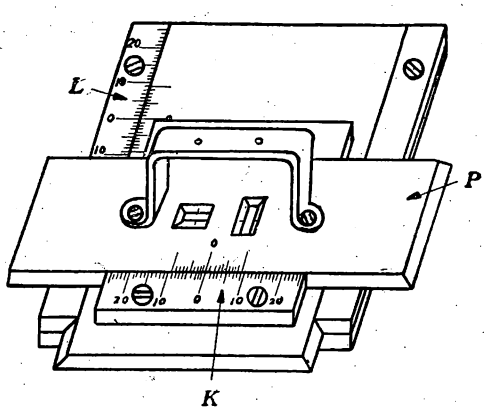

Fig. 6.
The Measuring Plate.

III. Materials Used and Forms of Specimens Employed.

The test pieces of the materials used in the present experiments were of the following four kinds of metals:

(1) Swedish hard steel received in the form of a bar 25 mm in diameter and about 3.65 m in length. This material is denoted "982 FA".

(2) Mild steel received in the form of a bar 36 mm in diameter and about 3.65 m in length. This material is denoted "5695".

(3) Gray cast iron bars made in the laboratory. This material is denoted "IC2".

(4) Duralumin received in the form of a bar 30 mm in diameter and about 4 m in length. This material is denoted "D-30".

The both ends about 10 cm in length were

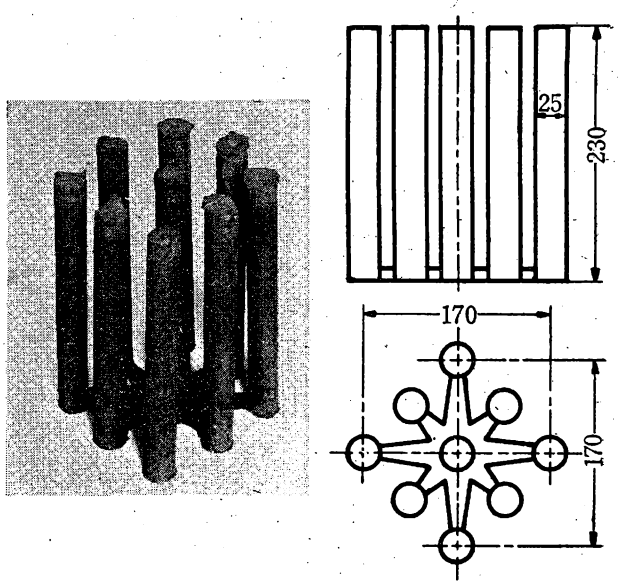

Fig. 7.
Moulding Shape of Cast Iron.

rejected from each bar in the testing experiments. The hard steel and the mild steel samples were subjected to the experiments as they were received and without any heat treatment in the laboratory. Special attention was given to the moulding shape of cast iron, as it exerts influence upon the properties of cast iron. As shown in Fig. 7, eight rods of about 25 mm in diameter and 230 mm in length were made as one casting. The duralumin sample was the one quenched and age-hardened after extrusion.

Chemical analysis was carried out on every material. The results are shown in Table 1. A microscopical examination was also made on samples of all the materials used. Fig. 8 shows the results.

In order to ascertain the mechanical properties of the materials, complete tests of static tension to destruction were made on two specimens of each

Table 1.

Chemical Composition of Materials.

Material	Symbol	Chemical Composition in %								
		C	Mn	S	P	Si	Fe	Al	Mg	Cu
Hard Steel	982 FA	0.51	0.38	0.010	0.023	0.27				
Mild Steel	5695	0.10	0.50	0.040	0.033	0.14				
Cast Iron	IC 2	Total 3.871 Graphitic 3.043	0.540	0.105	0.490	1.672				0.040
Duralumin	D-30		0.44			0.35	0.38		0.42	3.81

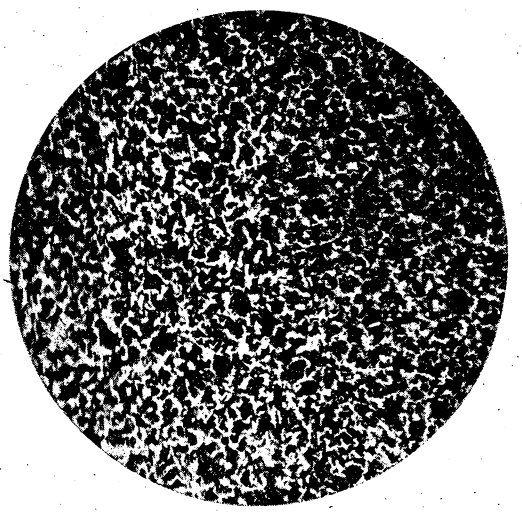

Hard Steel ×100

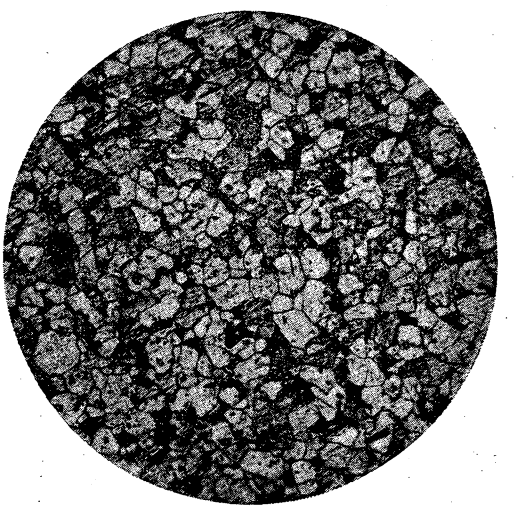

Mild Steel ×100

Cast Iron ×100

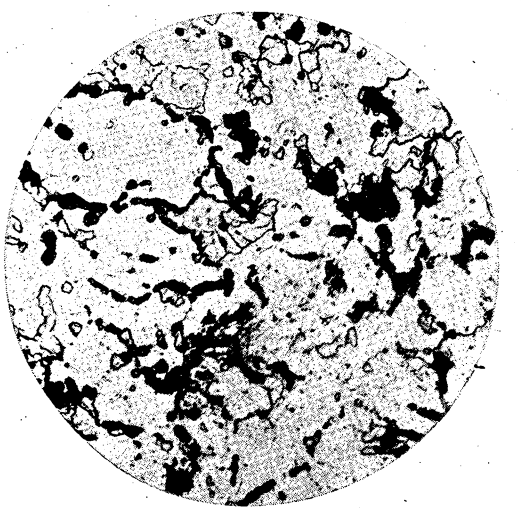

Duralumin ×100

Fig. 8.

Microscopical Structure of Materials.

Table 2.

Mechanical Properties of Materials.

Material	Symbol	Heat Treatment	Upper Yield Point, kg/mm²	Lower Yield Point, kg/mm²	Ultimate Strength, kg/mm²	Breaking Stress on Final Area, kg/mm²	Elongation, %	Reduction of Area, %	Brinell Hardness Number
Hard Steel	982FA	Hot-rolled	41.7 42.0	40.0 40.0	69.4 69.5	107.1 109.3	29.8 28.7	44.6 45.6	185 189
Mild Steel	5695	Hot-rolled	26.5 30.1	22.6 22.7	38.2 38.1	83.5 83.1	44.6 41.6	68.0 67.7	101 101
Cast Iron	IC2	Cast			19.4 17.5				179 178
Duralumin	D-30	Extruded, quenched	31.2 30.6		44.6 43.7	52.8 53.4	15.0 14.3	21.7 20.8	97.1 97.5

material. The form and dimensions of the tensile specimen are shown in Fig. 9 (a). The results of static tests are summarized in Table 2. In the tension tests of two carbon steels, the yield points were clearly observed. In duralumin, however, there was no marked drop of load at yield points, so the strain measurements were made by means of a mirror extensometer of the Martens type, and the yield points were decided from the stress-strain diagrams thus obtained as the point of 0.2 per cent permanent set. Brinell hardness tests were also made on two specimens of each material, and the results are given in Table 2.

(a) Tensile Specimen

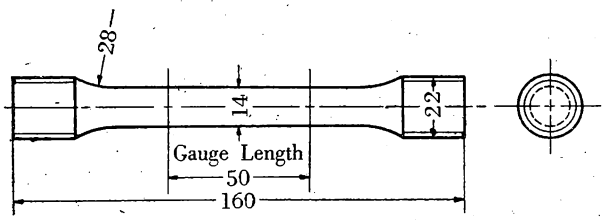

(b) Combined Stress Fatigue Specimen

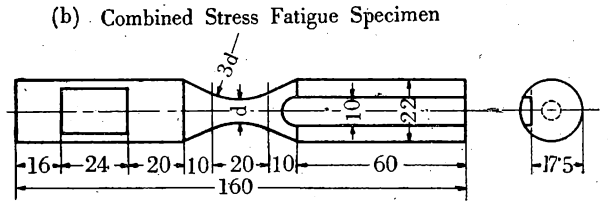

d=8 mm for hard and mild steels
d=10 mm for cast iron
d=11 mm for duralumin

Fig. 9.
Test Specimen.

The form and dimensions of the specimens employed for fatigue test are shown in Fig. 9 (b). The fatigue specimens have no parallel part, but have the fillet of radius thrice the diameter of the slenderest part. The diameter of the fatigue specimen must be chosen appropriately according to each material. If the diameter is too large the alternating moment to be applied becomes over the capacity of the testing machine, and if it is too small, it is impossible to make experiments, because the resonant or critical speed of the fly wheel becomes below the driving speed of the testing machine. (The testing machine should not of course be operated at a speed over the resonant or critical one. In the experiments described here it was kept in most cases at 1140 stress cycles per minute, though the resonant speed was sometimes far higher.) Consequently, the diameter of the specimen was chosen as 8 mm for steel, 10 mm for cast iron and 11 mm for duralumin. Further it must be noted that the specimen is to be attached to the testing machine in such a way as the slenderest part is in accord with xx-axis. (See Fig. 1 (a).)

IV. Description of the Combined Stresses and the Test Results Obtained.

Owing to the inertia forces of the fly wheel, the range of bending moment $\pm M_b$ and the range of torsional moment $\pm M_t$ are applied to the specimen. Then the maximum bending stress σ_a and the maximum torsional stress τ_a are induced in the specimen:

$$\sigma_a = \frac{32}{\pi d^3} M_b$$

$$\tau_a = \frac{16}{\pi d^3} M_t$$

The maximum principal stress σ_{max} and the maximum shear stress τ_{max}, which are induced by the combination of those bending and torsional stresses, are as follows:

when bending and torsional stresses are in phase,

$$\sigma_{max} = \frac{1}{2}\sigma_a + \frac{1}{2}\sqrt{\sigma_a^2 + 4\tau_a^2} \qquad (4)$$

$$\tau_{max} = \frac{1}{2}\sqrt{\sigma_a^2 + 4\tau_a^2} \qquad (5)$$

and when bending and torsional stresses are not in phase,

$$\sigma_{\max}=\left[\frac{1}{2}\sigma_a\cos\omega t+\frac{1}{2}\sqrt{\sigma_a^2\cos^2\omega t+4\tau_a^2\cos^2(\omega t-\delta)}\right]_{\max} \quad (6)$$

$$\tau_{\max}=\left[\frac{1}{2}\sqrt{\sigma_a^2\cos^2\omega t+4\tau_a^2\cos^2(\omega t-\delta)}\right]_{\max} \quad (7)$$

where ω is angular velocity, t is time, and δ is the angle of phase difference between bending and torsion. The time t in eqnation (6) or (7) must be determined as the value of the inside of the brackets becomes maximum. And the time t when the inside of the bracket is made maximum varies with the value of the ratio of σ_a to τ_a and also with the phase difference δ.

As it is rather tedious to calculate the values of $\sigma_{\max}$ and $\tau_{\max}$ from the relations (6) and (7), let us, for convenience' sake, use equations (4) and (5), even when the bending and torsional stresses are not in phase. Let the values of the stresses, thus calculated, be $\sigma_{n\,\max}$ and $\tau_{n\,\max}$: then

$$\sigma_{n\,\max}=\frac{1}{2}\sigma_a+\frac{1}{2}\sqrt{\sigma_a^2+4\tau_a^2} \quad (8)$$

$$\tau_{n\,\max}=\frac{1}{2}\sqrt{\sigma_a^2+4\tau_a^2} \quad (9)$$

where σ_a and τ_a are not in phase. Of course, the stress $\sigma_{n\,\max}$ or $\tau_{n\,\max}$ is not a value in real existence but only a nominal one which is generally greater than the true value of the maximum principal stress or the maximum shear stress. In the special case when the phase difference becomes zero or when either stress, σ_a or τ_a, becomes zero, the nominal stress represents the true stress.

In the experiments described here, we have carried out endurance tests at the following five combinations of bending and torsional stresses: that is, putting

$$\tan\theta=\frac{M_b}{M_t}=\frac{\sigma_a}{2\tau_a},$$

we took 0, 22.5, 45, 67.5 and 90 degrees as the values of θ. As already mentioned, when θ is 0 degree, it corresponds to the case in which only the torsional stress is working, and when θ it 90 degrees, it corresponds to the case in which only the bending stress is working. These relations are analogous to the relations in our previous report.

Under these conditions of the stress combination, phase difference was applied upon the bending and torsional stresses. The magnitudes of the phase difference were taken as 0, 30, 60 and 90 degrees of the value of δ. Occasionally the cases of 30 or 60 degrees were omitted. When δ is 0 degree, it corresponds to the case where both bending and torsional stresses are in phase, and δ is made 90 degrees, either bending or torsional stress disappears at the instant when the other stress takes the maximum value. It is of no need to consider the cases, in which phase difference is more than 90 degree or less than 0 degree, as those cases can be reduced always to the similar cases where it is between 0 and 90 degrees.

At the endurance tests we applied a little more than ten millions of stress repetitions to the unbroken specimen to determine the fatigue limit, though it was desirable for duralumin to apply a much greater stress cycles such as a hundred million or more. The results of the endurance tests are as follows:

(1) *Hard Steel.*

As previously mentioned, experiments were carried out under five stress combinations of bending and torsion, i.e., θ=0, 22.5, 45, 67.5, and 90 degrees. As the cases with phase difference, tests were made on three cases of δ=30, 60, and 90 degrees when θ=22.5 and 45 degrees, and on a single case of δ=90 degrees when θ=67.5 degrees.

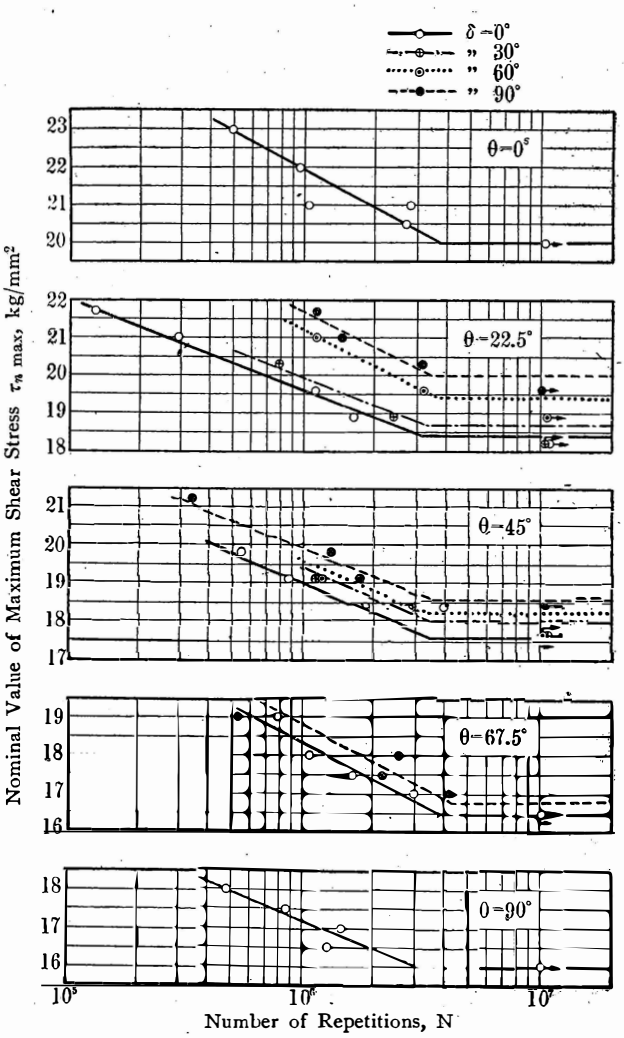

Fig. 10.
Stress-Endurance Diagrams for Hard Steel.

Table 3.

Results of Combined Stress Fatigue Tests on Hard Steel.

Test Piece No.	θ deg.	δ deg.	Nominal Value of Maximum Shear Stress $\tau_{n\,max}$, kg/mm²	Amplitude of Direct Stress due to Bending σ_a, kg/mm²	Amplitude of Shear Stress due to Torsion τ_a, kg/mm²	Number of Repetitions N, 10^6	Remarks
HNK 50	0	—	23.0	0	23.0	0.495	Broken
,, 47			22.0	,,	22.0	0.951	,,
,, 57			21.0	,,	21.0	1.043	,,
,, 49			,,	,,	,,	2.816	,,
,, 54			20.5	,,	20.5	2.709	,,
,, 64			20.0	,,	20.0	10.419	Unbroken
,, 74	22.5	0	21.7	16.60	20.05	0.127	Broken
,, 70			21.0	16.07	19.40	0.291	,,
,, 71			19.6	15.00	18.14	1.119	,,
,, 76			18.9	14.46	17.46	1.629	,,
,, 73			18.2	13.92	16.81	10.814	Unbroken
,, 97		30	20.3	15.53	18.75	0.785	Broken
,, 96			18.9	14.47	17.45	2.399	,,
,, 95			18.2	13.92	16.81	10.480	Unbroken
,, 84		60	21.0	16.07	19.40	1.129	Broken
,, 94			19.6	15.00	18.10	3.181	,,
,, 93			18.9	14.46	17.46	10.632	Unbroken
,, 67		90	21.7	16.60	20.05	1.129	Broken
,, 68			21.0	16.07	19.40	1.444	,,
,, 69			20.3	15.54	18.76	3.144	,,
,, 72			19.6	15.00	18.10	10.047	Unbroken
,, 60	45	0	19.8	28.0	14.0	0.541	Broken
,, 62			19.1	27.0	13.5	0.862	,,
,, 89			18.4	26.0	13.0	1.839	,,
,, 92			17.7	25.0	12.5	10.049	Unbroken
,, 98		30	19.1	27.0	13.5	1.131	Broken
,, 99			18.4	26.0	13.0	2.880	,,
,, 88			17.7	25.0	12.5	10.728	Unbroken
,, 90		60	19.1	27.0	13.5	1.198	Broken
,, 91			18.4	26.0	13.0	3.925	,,
,, 87			17.7	25.0	12 5	10.309	Unbroken
,, 59		90	21.2	30.0	15.0	0.334	Broken
,, 61			19.8	28.0	14.0	1.298	,,
,, 63			19.1	27.0	13.5	1.727	,,
,, 65			18.4	26.0	13.0	10.454	Unbroken
,, 79	67.5	0	19.0	35.10	7.27	0.771	Broken
,, 77			18.0	33.25	6.89	1.069	,,
,, 82			17.5	32.35	6.70	1.614	,,
,, 75			17.0	31.40	6.51	2.890	,,
,, 78			16.5	30.49	6.31	10.147	Unbroken
,, 83		90	19.0	35.10	7.27	0.528	Broken
,, 81			18.0	33.25	6.89	2.546	,,
,, 85			17.5	32.35	6.70	2.171	,,
,, 86			17.0	31.40	6.51	4.142	,,
,, 80			16.5	30.49	6.31	10.584	Unbroken
,, 53	90	—	18.0	36.0	0	0.479	Broken
,, 58			17.5	35.0	,,	0.857	,,
,, 52			17.0	34.0	,,	1.458	,,
,, 55			16.5	33.0	,,	1.270	,,
,, 51			16.0	32.0	,,	10.117	Unbroken

The test results are shown in Table 3. Fig. 10 is the stress-endurance diagram obtained from the test results. Fatigue limits were estimated from the stress-endurance diagram, and the values of fatigue limits obtained are summarized in Tabe 7.

(2) *Mild Steel.* –

In this case also tests were made under five stress combinations, i. e., $\theta=0$, 22.5, 45, 67.5, and 90 degrees. For the phase difference, two cases of $\delta=60$ and 90 degrees were adopted where $\theta=$ 22.5 and 45 degrees, and one single case of $\delta=90$ degrees where $\theta=67.5$ degrees. The test results are shown in Table 4 and Fig. 11 is the stress-endurance diagram obtained from them. Fatigue limits were estimated from the stress-endurance diagram, and the results are summarized in Table 7.

(3) *Cast Iron.*

Five stress combinations were adopted here also, i.e., $\theta=0$, 22.5, 45, 67.5, and 90 degrees. For the phase difference, the similar cases as with the mild steel were taken, i.e., two cases of $\delta=60$ and 90 degrees when $\theta=22.5$ and 45 degrees, and

Table 4.

Results of Combined Stress Fatigue Tests on Mild Steel.

Test Piece No.	θ deg.	δ deg.	Nominal Value of Maximum Shear Stress $\tau_{n\,max}$, kg/mm²	Amplitude of Direct Stress due to Bending σ_a, kg/mm²	Amplitude of Shear Stress due to Torsion τ_a, kg/mm²	Number of Repetitions N, 10^6	Remarks
LNK 1	0	—	17.0	0	17.0	0.123	Broken
„ 2			15.0	„	15.0	1.496	„
„ 11			14.5	„	14.5	5.196	„
„ 3			14.0	„	14.0	11.041	Unbroken
„ 16	22.5	0	13.5	10.33	12.47	5.323	Broken
„ 17			13.0	9.95	12.01	10.184	Unbroken
„ 40		60	14.5	11.10	13.40	2.160	Broken
„ 36			14.0	10.72	12.93	1.164	„
„ 37			13.5	10.33	12.47	10.918	Unbroken
„ 25		90	15.5	11.86	14.32	0.790	Broken
„ 27			15.0	11.48	13.86	1.645	„
„ 26			14.5	11.10	13.40	10.182	Unbroken
„ 12	45	0	13.5	19.09	9.54	2.253	Broken
„ 13			13.0	18.38	9.19	10.637	Unbroken
„ 31		60	14.5	20.50	10.25	2.734	Broken
„ 32			14.0	19.80	9.90	4.915	„
„ 33			13.5	19.09	9.54	10.000	Unbroken
„ 22		90	17.0	24.04	12.02	0.182	Broken
„ 41			16.0	22.62	11.31	2.608	„
„ 24			15.0	21.21	10.61	1.635	„
„ 21			14.5	20.50	10.25	11.094	Unbroken
„ 18	67.5	0	13.0	24.02	4.98	1.312	Broken
„ 20			12.3	22.73	4.71	10.111	Unbroken
„ 19			12.0	22.17	4.59	10.374	„
„ 28		90	13.5	24.95	5.17	0.592	Broken
„ 29			13.0	24.02	4.98	4.726	„
„ 30			12.5	23.10	4.78	10.172	Unbroken
„ 5	90	—	15.0	30.0	0	0.108	Broken
„ 6			13.5	27.0	„	0.944	„
„ 7			13.0	26.0	„	1.470	„
„ 35			12.5	25.0	„	1.419	„
„ 38			12.0	24.0	„	10.036	Unbroken
„ 10			11.5	23.0	„	10.084	„
„ 9			11.0	22.0	„	11.028	„

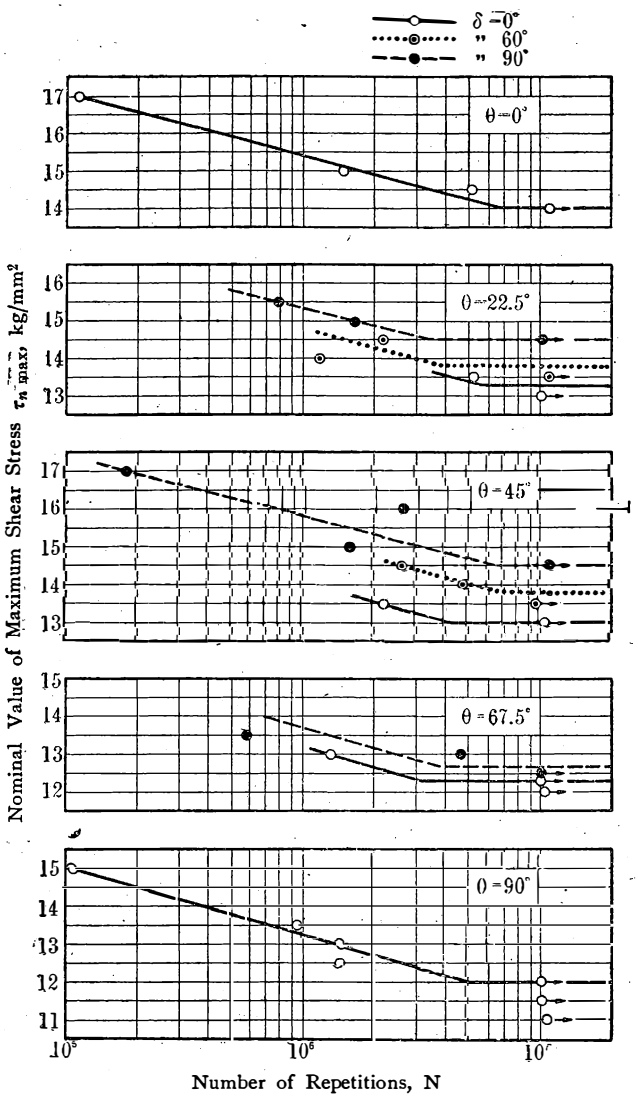

Fig. 11.
Stress-Endurance Diagrams for Mild Steel.

one single case of $\delta=90$ degrees when $\theta=67.5$ degrees. The test results are shown in Table 5 and the stress-endurance diagram in Fig. 12. Values of fatigue limits were estimated from the stress-endurance diagram and are summarized in Table 7.

(4) *Duralumin.*

Three stress combinations were adopted here, i.e., $\theta=0$, 45, and 90 degrees. For the phase

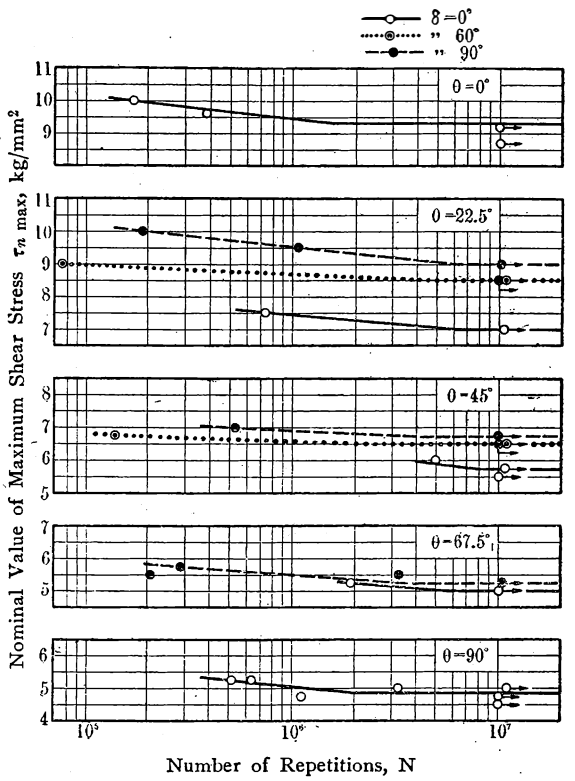

Fig. 12.
Stress-Endurance Diagrams for Cast Iron.

Table 5.

Results of Combined Stress Fatigue Tests on Cast Iron.

Test Piece No.	θ deg.	δ deg.	Nominal Value of Maximum Shear Stress $\tau_{n\,max}$, kg/mm²	Amplitude of Direct Stress due to Bending σ_a, kg/mm²	Amplitude of Shear Stress due to Torsion τ_a, kg/mm²	Number of Repetitions N, 10^6	Remarks
CNK 36	0	—	10.0	0	10.0	0.170	Broken
" 1			9.6	"	9.6	0.383	"
" 35			9.2	"	9.2	10.047	Unbroken
" 3			8.7	"	8.7	10.009	"
" 23	22.5	0	7.5	5.74	6.93	0.744	Broken
" 22			7.0	5.36	6.47	10.432	Unbroken
" 33		60	9.0	6.89	8.32	0.077	Broken
" 32			8.5	6.50	7.85	10.747	Unbroken
" 38		90	10.0	7.65	9.24	0.188	Broken
" 39			9.5	7.27	8.78	1.076	"
" 37			9.0	6.89	8.32	10.115	Unbroken
" 26			8.5	6.50	7.85	10.000	"

„ 7			6.0	8.50	4.24	4.870	Broken
„ 20		0	5.75	8.13	4.06	10.554	Unbroken
„ 8			5.5	7.80	3.90	10.000	„
„ 30	45	60	6.75	9.55	4.78	0.136	Broken
„ 31			6.5	9.20	4.60	10.820	Unbroken
„ 10			7.0	9.90	4.95	0.538	Broken
„ 21		90	6.75	9.55	4.77	10.000	Unbroken
„ 11			6.5	9.20	4.60	10.000	„
„ 12		0	5.25	9.70	2.01	1.902	Broken
„ 13			5.0	9.24	1.91	10.036	Unbroken
„ 16	67.5		5.75	10.62	2.20	0.290	Broken
„ 18		90	5.5	10.15	2.10	0.205	„
„ 19			„	„	„	3.237	„
„ 17			5.25	9.70	2.01	10.447	Unbroken
„ 4			5.25	10.5	0	0.634	Broken
„ 28			„	„	„	0.504	„
„ 14			5.0	10.0	„	3.244	„
„ 29	90	—	„	„	„	10.764	Unbroken
„ 6			4.75	9.5	„	1.101	Broken
„ 15			„	„	„	10.000	Unbroken
„ 5			4.5	9.0	„	10.045	„

Table 6.

Results of Combined Stress Fatigue Tests on Duralumin.

Test Piece No.	θ deg.	δ deg.	Nominal Value of Maximum Shear Stress $\tau_{n\,max}$, kg/mm²	Amplitude of Direct Stress due to Bending σ_a, kg/mm²	Amplitude of Shear Stress due to Torsion τ_a, kg/mm²	Number of Repetitions N, 10^6	Remarks
DNK 5			13.0	0	13.0	1.093	Broken
„ 4			11.0	„	11.0	3.771	„
„ 3	0	—	10.5	„	10.5	8.626	„
„ 2			10.0	„	10.0	10.695	„
„ 1			9.5	„	9.5	10.048	Unbroken
„ 20	22.5	0	11.0	8.42	10.16	1.086	Broken
„ 24		90	„	„	„	2.147	„
„ 12	45	0	11.0	15.55	7.78	1.315	„
„ 11			9.5	13.43	6.72	3.183	„
„ 16			9.0	12.73	6.37	6.758	„
„ 15		90	10.0	14.14	7.07	2.669	„
„ 19			8.5	12.02	6.01	5.672	„
„ 22	67.5	0	11.0	20.33	4.21	0.607	„
„ 17			9.0	16.63	3.44	2.286	„
„ 23		90	11.0	20.33	4.21	1.461	„
„ 8			10.0	18.48	3.83	1.719	„
„ 7	90	—	10.0	20.0	0	0.835	„
„ 10			9.0	18.0	„	1.646	„
„ 9			8.5	17.0	− „	2.302	„
„ 6			8.0	16.0	„	8.263	„
„ 13			7.5	15.0	„	10.305	Unbroken

Table 7.
Summary of Fatigue Limits for All Materials.

Material	θ deg.	δ deg.	Nominal Value of Maximum Shear Stress $\tau_{n\,max}$, kg/mm²	Amplitude of Direct, Stress due to Bending σ_a, kg/mm²	Amplitude of Shear Stress due to Torsion τ_a, kg/mm²	Rate of Increase due to Phase Difference, %
Hard Steel	0	—	20.0	0	20.0	—
	22.5	0	18.4	14.08	17.00	0
		30	18.7	14.31	17.28	1.6
		60	19.4	14.85	18.01	5.4
		90	20.0	15 31	18.48	8.7
	45	0	17.7	25.00	12.50	0
		30	18.0	25.45	12.73	1.7
		60	18.2	25.73	12.87	2.8
		90	18.6	26.30	13.15	5.1
	67.5	0	16.5	30.49	6.31	0
		90	16.8	31.04	6.43	1.8
	90	—	16.0	32.00	0	—
Mild Steel	0	—	14.0	0	14.00	—
	22.5	0	13.3	10.18	12.29	0
		60	13.8	10.56	12.75	3.8
		90	14.5	11.10	13.40	9.0
	45	0	13.0	18.38	9.19	0
		60	13.8	19.51	9.76	6.2
		90	14.5	20.50	10.25	11.5
	67.5	0	12.3	22.73	4.71	0
		90	12.7	23.47	4.86	3.3
	90	—	12.0	24.00	0	—
Cast Iron	0	—	9.3	0	9.30	—
	22.5	0	7.0	5.36	6.47	0
		60	8.5	6.50	7.85	21.4
		90	9.0	6.89	8.32	28.6
	45	0	5.75	8.13	4.06	0
		60	6.5	9.20	4.60	13.0
		90	6.75	9.55	4.77	17.4
	67.5	0	5.0	9.24	1.91	0
		90	5.25	9.70	2.01	5.0
	90	—	4.9	9.80	0	—
Duralumin	0	—	10.2	0	10.2	—
	45	0	8.7	12.30	6.15	0
		90	"	"	"	"
	90	—	7.95	15.90	0	—

difference, there was adopted only a single case of $\delta=90$ degrees at the value of $\theta=45$ degrees. The test results are shown in Table 6 and the stress-endurance diagram is given in Fig. 13. Fatigue limits were estimated from the stress-endurance diagram as the values for 10^7 stress repetitions and is summarized in Table 7. To see the fatigue fractures of duralumin, experiments were made on some specimens at $\delta=0$ and 90 degrees for $\theta=22.5$ degrees, at $\delta=60$ degrees for $\theta=45$ degrees, and $\delta=0$ and 90 degrees for $\theta=67.5$ degrees.

In the above tables, the applied stresses are mentioned in the calculated values of the direct and shear stresses due to bending and twisting moments respectively, and also of the nominal values of the maximum shear stresses. In the

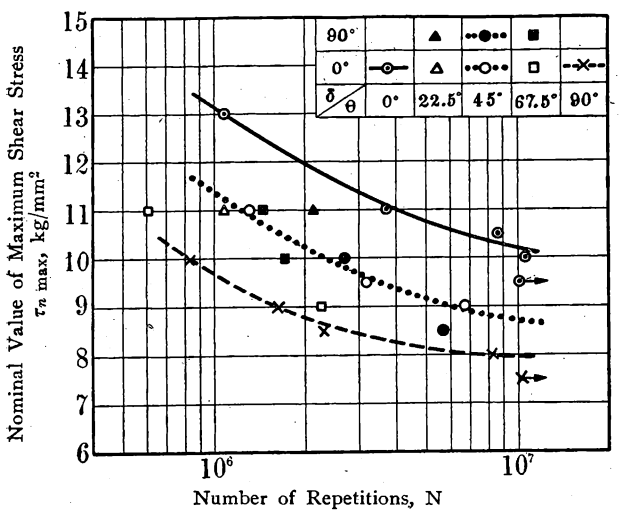

Fig. 13.
Stress-Endurance Diagram for Duralumin.

above stress-endurance diagrams, the nominal value of the maximum shear stress is always taken as the ordinate.

V. Consideration of the Experimental Results.

(1) *Comparison of test results with the criterion on fatigue failure.*

(a) When bending and torsional stresses are in phase.

Let us consider first the case where bending and torsional stresses are in phase. In examining the test results, it is convenient to show the results in diagrams — σ_a–τ_a diagrams — taking the amplitude of direct stress due to bending as abscissa and the amplitude of shear stress due to torsion as ordinate. Fig. 14 shows the σ_a–τ_a diagrams obtained for all the materials. Where

σ_a = amplitude of direct stress due to bending
τ_a = amplitude of shear stress due to torsion
} at the fatigue limit of the combination.

σ_w = fatigue limit in pure bending.

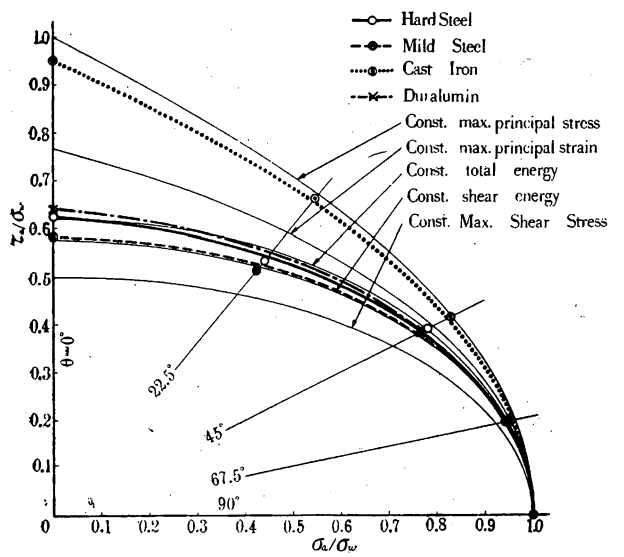

Fig. 14.
σ_a–τ_a Diagrams—when bending and torsional stresses are in phase.

In Fig. 14 are represented the amplitudes of direct and shear stresses in both coordinate axes by the ratios of those values to σ_w. Therefore all the results shown in Fig. 14 are necessarily in accord with one another at the point of σ_w on σ_a-axis. In σ_a–τ_a diagram, the results under reversed bending (i. e., θ=90 degrees) and reversed torsion (i. e., θ=0 degrees) are plotted respectively on σ_a and τ_a-axes, while the results under combined bending and torsion, having any definite value of θ, are plotted on a radial line having an included angle $\tan^{-1}(2\tan\theta)$ with τ_a-axis.

In a previous report,[5] the authors have proposed a new criterion on the strength of metals under combined alternating bending and torsion. According to it, the conditions of fatigue failure are represented by the following expressions when bending and torsional stresses are in phase:

(i) When $\varphi \leqslant 1/\sqrt{3}$

$$\sigma_a^2 + \frac{1}{\varphi^2}\tau_a^2 = \sigma_w^2 \qquad (10)$$

(ii) When $\varphi > 1/\sqrt{3}$

$$(1+\varphi^2)\sigma_a^2 + (3\varphi^2-1)\sigma_a\sqrt{\sigma_a^2+4\tau_a^2} + 4\tau_a^2 = 4\varphi^2\sigma_w^2 \qquad (11)$$

or simply

$$(1-\varphi^2)\sigma_a^2 + (3\varphi^2-1)\sigma_w\sigma_a + 2\tau_a^2 = 2\varphi^2\sigma_w^2 \qquad (12)$$

where

$\varphi = \tau_w/\sigma_w$
σ_w = fatigue limit in pure bending
τ_w = " " " " torsion

Applying this criterion to the present experiments, the values of σ_w, τ_w and φ for each material are as shown in Table 8. Applying the values of σ_w and φ in equation (10) or (12), we obtain the conditions of fatigue failure, which are shown with thick lines in Fig. 14. It is seen that these curves are in good agreement with the test results.

For reference, let us also compare the results of experiments with some other criterions concerning the elastic failure of metals under static stresses; i. e., the criterions of constant maximum shear stress, of constant maximum principal strain, of constant

(5) T. Nishihara and M. Kawamoto, "A New Criterion for the Strength of Metals under Combined Alternating Stresses." Memoirs of the College of Engineering, Kyoto Imperial University, Vol. XI, No. 4 (1944), p. 70.

Table 8.
Value of φ.

Material	Fatigue Limit in Pure Bending σ_w, kg/mm²	Fatigue Limit in Pure Torsion τ_w, kg/mm²	φ
Hard Steel	32.0	20.0	0.625
Mild Steel	24.0	14.0	0.583
Cast Iron	9.8	9.3	0.949
Duralumin	15.9	10.2	0.642

total strain energy, of constant shear strain energy, and of constant maximum shear stress. Applying these criterions which have been already mentioned in the previous report to the case considered here, we obtain the curves shown with thin lines in Fig. 14, where Poisson's constant is put as 10/3. As seen in Fig. 14, these criteria are not in as good an agreement with the test results as with the authors' criterion. Thus the good applicability of the latter criterion to experimental results is proved again in the present experiments.

(b) When bending and torsional stresses are not in phase.

In examining the test results where bending and torsional stresses are not in phase, it is also convenient to show them in σ_a–τ_a diagrams, which are, in Figs. 15~18, drawn from the test results.

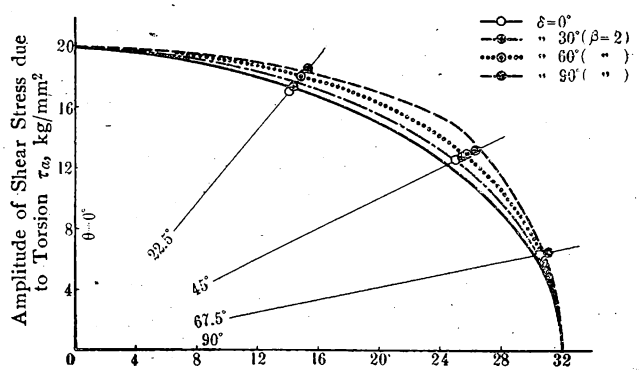

Fig. 15.
σ_a–τ_a Diagram for Hard Steel.

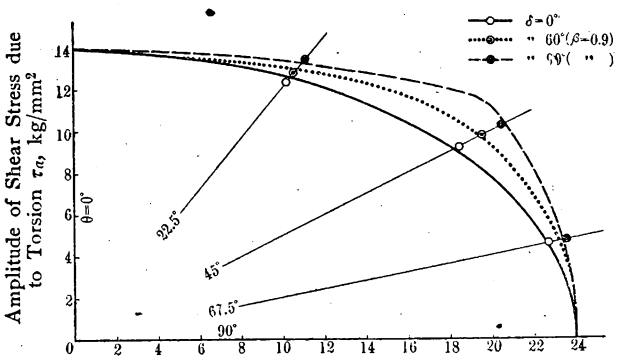

Fig. 16.
σ_a–τ_a Diagram for Mild Steel.

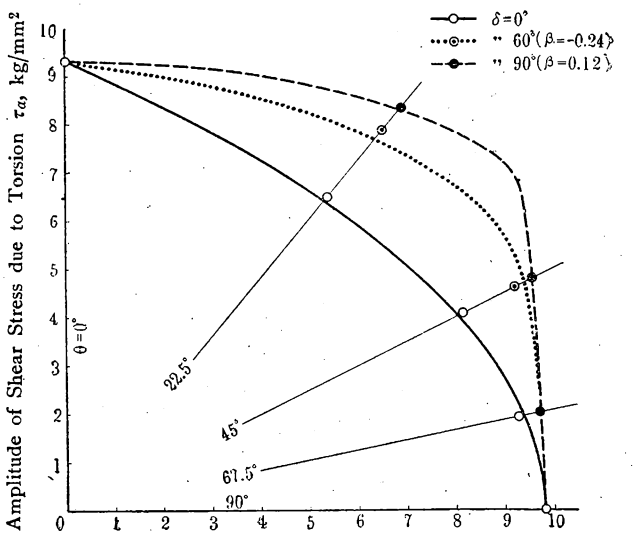

Fig. 17.
σ_a–τ_a Diagram for Cast Iron.

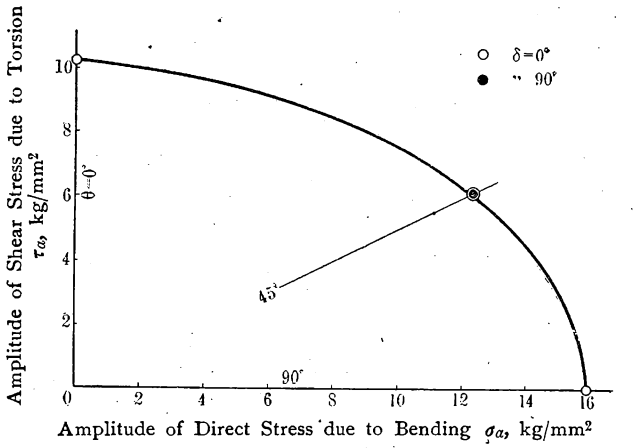

Fig. 18.
σ_a–τ_a Diagram for Duralumin.

In the previous report the authors have derived the equations representing the conditions of fatigue failure under alternating stresses with phase difference, but they could not examine their applicability because at that time there were no experimental results concerning the fatigue resistance under combined stresses with phase difference. Now, however, we can examine it.

The conditions of fatigue failure due to the authors' criterion, as given in the previous report, are as follows:

(i) When $\varphi \leqq 1/\sqrt{3}$

$$\left.\begin{aligned} \sigma_a &= \sqrt{\frac{1+\beta}{h_1+(1+h_2)\beta}}\,\sigma_w \\ \tau_a &= \sqrt{h_2}\,\varphi\sigma_a \end{aligned}\right\} \quad (13)$$

where

$$\left.\begin{aligned} h_1&=\cos^2 i\delta+\sin i\delta\cos i\delta\,\frac{\cos(1-i)\delta}{\sin(1-i)\delta}\\ h_2&=\frac{\sin i\delta\cos i\delta}{\sin(1-i)\delta\cos(1-i)\delta}\end{aligned}\right\}\quad(14)$$

Considering i as a parameter in these equations, we can obtaine the relation between σ_a and τ_a at the fatigue limit of the combination for an arbitrary value of δ when σ_w and φ are given. But we cannot obtaine the relation between σ_a and τ_a from equations (13) and (14), when the angle of phase difference δ is equal to 90 degrees. In this case the relations between σ_a and τ_a becomes

$$\left.\begin{aligned} &\sigma_a^2+\frac{\beta}{1+\beta}\frac{1}{\varphi^2}\tau_a^2=\sigma_w^2 \quad\text{when}\quad \sigma_a\geqq\frac{1}{\varphi}\tau_a\\ &\frac{\beta}{1+\beta}\sigma_a^2+\frac{1}{\varphi^2}\tau_a^2=\sigma_w^2 \qquad\qquad \sigma_a\leqq\frac{1}{\varphi}\tau_a\end{aligned}\right\}\quad(15)$$

(ii) When $\varphi>1/\sqrt{3}$

$$[(\varphi^2+1)\sigma_a^2\sin i\delta\cos i\delta-4\tau_a^2\sin(1-i)\delta\cos(1-i)\delta]\sqrt{\sigma_a^2\cos^2 i\delta+4\tau_a^2\cos^2(1-i)\delta}+(3\varphi^2-1)\sigma_a[\sigma_a^2\sin i\delta\cos^2 i\delta+2\tau_a^2\{\sin i\delta\cos^2(1-i)\delta-\cos i\delta\sin(1-i)\delta\cos(1-i)\delta\}]=0 \quad(16)$$

$$(\varphi^2+1)\sigma_a^2\cos^2 i\delta+(3\varphi^2-1)\sigma_a\cos i\delta\sqrt{\sigma_a^2\cos^2 i\delta+4\tau_a^2\cos^2(1-i)\delta}+4\tau_a^2\cos^2(1-i)\delta+\beta[(\varphi^2+1)\sigma_a^2+(3\varphi^2-1)\sigma_a\sqrt{\sigma_a^2+4\tau_a^2}+4\tau_a^2]=4(1+\beta)\varphi^2\sigma_w^2 \quad(17)$$

Considering i as a parameter in equations (16) and (17), we can calculate values of σ_a and τ_a at the fatigue limit of the combination for an arbitrary value of δ, when σ_w and φ are given. But when angle of phase difference δ is equal to 90 degrees and σ_a is greater than $\frac{2}{\sqrt{\varphi^2+1}}\tau_a$, the relation between σ_a and τ_a becomes simply

$$4\varphi^2\sigma_a^2+\beta[(\varphi^2+1)\sigma_a^2+(3\varphi^2-1)\sigma_a\sqrt{\sigma_a^2+4\tau_a^2}+4\tau_a^2]=4(1+\beta)\varphi^2\sigma_w^2 \quad(18)$$

In the above equations β is a constant depending not only on material but also on phase difference of the applied stresses and it must be determined by experiments in each ease. Now assuming the value of β as shown in Table 9, we have drawn in Fig. 15~18 the curves which are represented by the above criterion. As seen in these figures, the curves are in good accordance with the test results, proving again the authors' criterion to be satisfactorily applicable also when the stresses are not in phase.

Table 9.

Value of β.

Material	Value of δ in degree		
	90	60	30
Hard Steel	2	2	2
Mild Steel	0.9	0.9	—
Cast Iron	0.12	−0.24	—
Duralumin	∞	—	—

(6) See foot-note (5).

(2) Effect of phase difference upon the fatigue resistance.

In examining the effect of phase difference, it is convenient to consider the value of constant β in the authors' criterion. This value depends, as already mentioned, not only on the material but also on phase difference of the applied stresses. About the effect of its magnitude upon the fatigue limit calculated from the authors' criterion a full consideration has been made in the previous report[6]. When β is infinity, the material is completely insensitive for phase difference, i. e., values of σ_a and τ_a at the fatigue limit become constant no matter whether the phase difference exists or not. And as the value of β decreases from infinity to zero, those of σ_a and τ_a gradually increase. And when β becomes negative, σ_a and τ_a increase still farther. Therefore the value of β can be considered in its physical meaning to represent the degree of insensibility for phase difference. If the value of β is obtained from experiments in each case, the effect of phase difference is of course made fully clear.

(a) On hard and mild steels.

The rates of increase of the values of σ_a, τ_a and $\tau_{n\,\max}$ due to phase difference are calculated and given in Table 7, and also shown in Fig. 19. According to the results, it is found that the rate of the increase due to phase difference takes the maximum values when $\theta=22.5$ degrees for hard steel and $\theta=45$ degrees for mild steel, and that the maximum values are roughly equal to 10 per cent.

Attention must be paid to the fact that the values of β for hard and mild steels in Table 9 are independent of phase difference, i. e., $\beta=2$ for the hard steel, and $\beta=0.9$ for the mild steel. If we may ascertain from these results that the value of β for steel is always independent of phase difference, a very informative result can be obtained. That is, in obtaining the effect of phase difference upon the fatigue resistance of steel, it is not necessary to make experiments for various values of δ, but sufficient to make experiments only for the case when $\delta=90$ degrees. But the value of β is different in each material.

(b) On cast iron.

The rates of increase of the fatigue limit due to phase difference are given in Table 7, and also

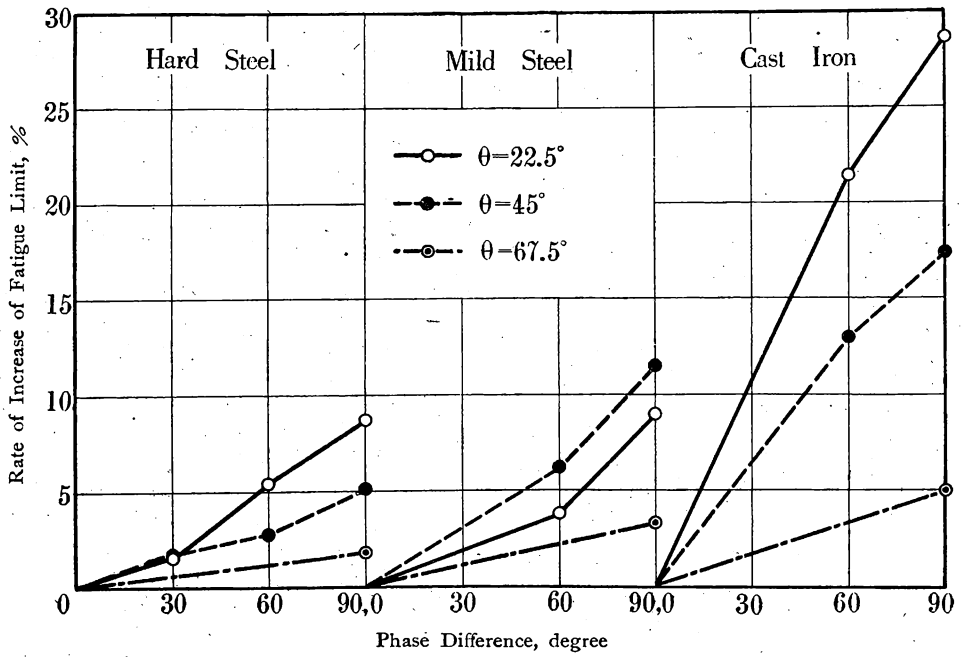

Fig. 19.
Rate of Increase of Fatigue Limit due to Phase Difference.

shown in Fig. 19. The maximum value of the rate of the increase occurs when $\theta=22.5$ degrees, and it reaches almost to 30 per cent. Thus the rate of the increase is very large in cast iron. Accordingly the value of β becomes very small, as shown in Table 9. Especially when $\delta=60$ degrees, β becomes negative. Attention must be paid to the results that the value of β for cast iron is not independent of phase difference, but smaller at $\delta=60$ degrees than at $\delta=90$ degrees. Therefore it is known that cast iron is very sensitive to phase difference, and the degree of sensitivity is large especially when phase difference is not large. The authors believe that these characteristics are the general properties of brittle materials.

(c) On duralumin.

In duralumin the fatigue limit does not increase with phase difference. As seen from the values in Table 7, it is, for the case without phase difference, approximately equal to that for the case with phase difference, when we take the fatigue limit as the value for 10^7 stress repetitions. That is, duralumin is completely insensitive for phase difference and its value of β must be infinity. However, in treating the fatigue resistance of duralumin in its true sense, we should apply much greater stress repetitions than 10^7. [Here it must be noted that the duralumin used in the present experiments had abnormal mechanical properties, that is, it seemed to have suffered the effect of extrusion to the highest degree and it had an extraordinary high static tensile strength as shown in Table 2.

(7) See foot-note (1).

VI. Fatigue Fractures.

It has been previously reported[7] that fatigue fractures always occur in regular directions according to the value of θ, when bending and torsional stresses are in phase. It is a very interesting and also instructive matter to investigate what appearance the fatigue fracture takes when the phase difference is applied to the combined stresses. By examining the directions of fracture planes of all the specimens that failed in the present experiments, a fair regularity could also be recognized.

(1) *Fractures of carbon steels and cast iron.*

The angle of inclination α of the fracture plane to the cross section of the specimen is measured for all the broken specimens of hard steel, mild steel, and cast iron. The measured angle α is summarized in Table 10.

It has been made clear already in the previous experiments that fatigue fracture of carbon steel and cast iron occurs always in the direction of the maximum principal stress due to combined stresses when they are in phase. The reason has been there considered to be in the fact that carbon steel is subjected to the hardening effect as the fatigue phenomena progresses and becomes more and more brittle and finally the fracture is caused by the maximum principal stress, as ordinarily in brittle materials.

Hereupon it will be supposed that when the combined stresses are not in phase, the fracture plane of carbon steel and cast iron should be

Table 10.

Inclination of Fracture Plane of Steel and Cast Iron to Cross Section of Specimen at point of maximum stress.

θ deg.	δ deg.	Hard Steel		Mild Steel		Cast Iron		Inclination of Plane of Maximum Principal Stress to Cross Section α', deg.
		Test Piece No.	Measured Angle α, deg.	Test Piece No.	Measured Angle α, deg.	Test Piece No.	Measured Angle α, deg.	
0	—	HNK 50	45	LNK 1	5	CNK 36	45	45
		„ 47	„	„ 2	10	„ 1	49(*)	
		„ 57	„	„ 11	45(*)			
		„ 49	„					
		„ 54	„ (*)					
22.5	0	„ 74	35	LNK 16	30(*)	CNK 23	34(*)	33.75
		„ 70	27					
		„ 71	33					
		„ 76	34(*)					
	30	„ 97	23					34.1
		„ 96	32(*)					
	60	„ 84	23	LNK 40	6	CNK 33	33(*)	35.45
		„ 94	22(*)	„ 36	22(*)			
	90	„ 67	24	„ 25	9	CNK 38	38	39
		„ 68	25	„ 27	39(*)	„ 39	37(*)	
		„ 69	28(*)					
45	0	„ 60	23	LNK 12	22(*)	CNK 7	25(*)	22.5
		„ 62	24					
		„ 89	22(*)					
	30	„ 98	15					21.6
		„ 99	17(*)					
	60	„ 90	7	LNK 31	7	CNK 30	17(*)	17.4
		„ 91	9(*)	„ 32	10(*)			
	90	„ 59	0(*)	„ 22	8	CNK 10	3(*)	0
		„ 61	„	„ 41	2(*)			
		„ 63	2	„ 24	4			
67.5	0	„ 79	12	„ 18	11(*)	CNK 12	11(*)	11.25
		„ 77	11(*)					
		„ 82	13					
		„ 75	11					
	90	„ 83	3	LNK 28	0(*)	CNK 16	0	0
		„ 81	2	„ 29	0	„ 18	6	
		„ 85	10			„ 19	0(*)	
		„ 86	1(*)					
90	—	„ 53	0	LNK 5	0	CNK 4	4	0
		„ 58	„	„ 6	1	„ 28	3	
		„ 52	„ (*)	„ 7	0(*)	„ 14	2	
		„ 55	„	„ 35	2	„ 6	0(*)	

Specimens with the mark (*) are shown in Figs. 21, 22, and 23.

consistent with the plane of the greatest maximum principal stress. Now let us calculate the angle of inclination of the plane of the greatest maximum principal stress to the cross section of the specimen. Let the angle be α', then

$$\tan 2\alpha' = \frac{2\tau_a \cos(\omega t - \delta)}{\sigma_a \cos \omega t} \qquad (19)$$

where time t should be taken when the maximum principal stress due to combined stresses becomes greatest, therefore

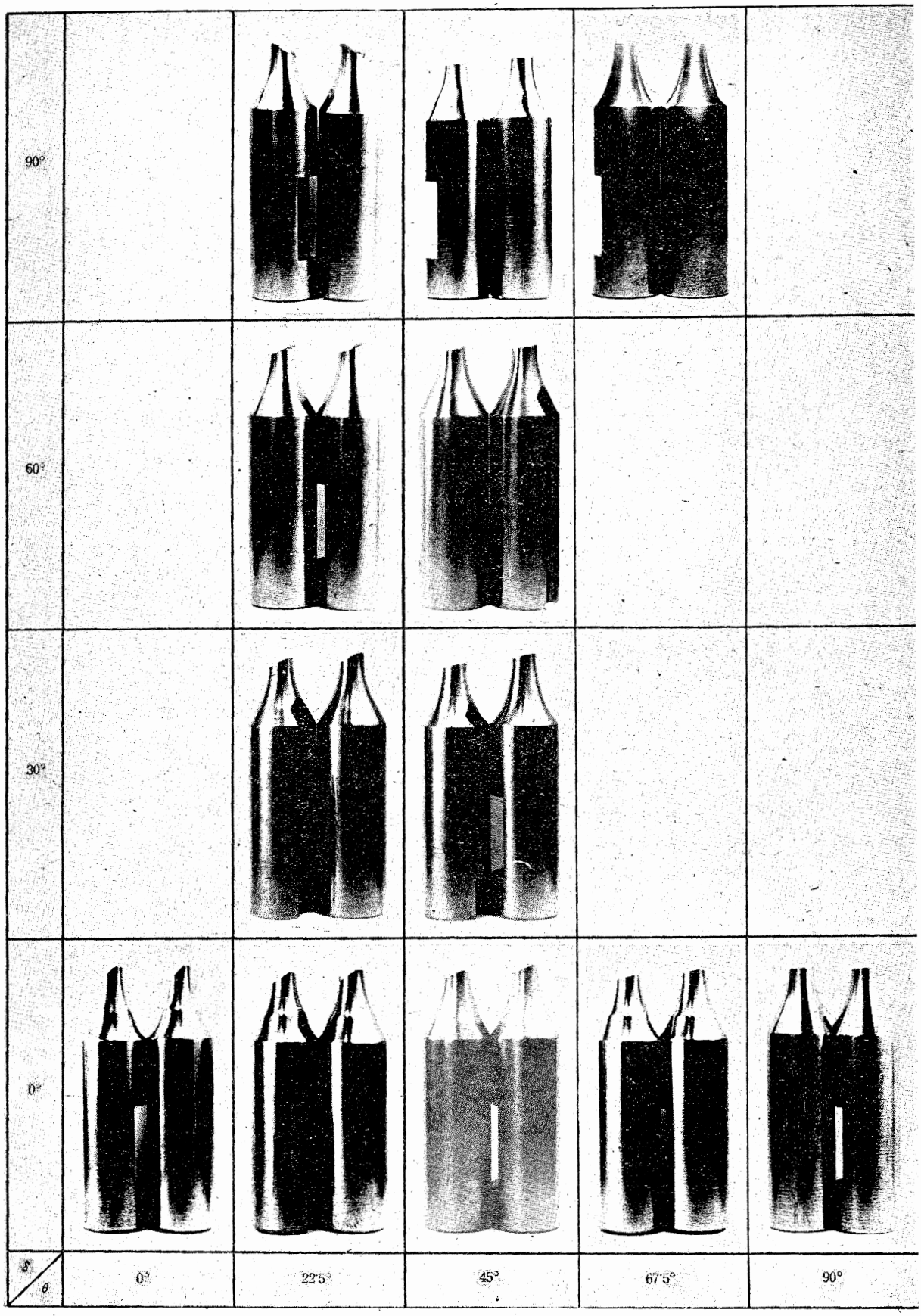

Fig. 20.

Fatigue Fractures of Hard Steel.

$$\frac{d}{dt}\left[\frac{1}{2}\sigma_a\cos\omega t+\frac{1}{2}\sqrt{\sigma_a^2\cos^2\omega t+4\tau_a^2\cos^2(\omega t-\delta)}\right]=0 \quad (20)$$

From equations (19) and (20) we can calculate the value of α', when the ratio of σ_a to τ_a (hence the value of θ) and the value of δ are given. The calculated values of α' are given in Table 10. As seen in the table, the value of α' becomes larger as the phase difference increases, when $\theta=22.5$ degrees. On the contrary, when $\theta=45$ and 67.5 degrees, the value of α' becomes smaller as the phase difference increases and finally it becomes zero at $\delta=90$ degrees.

Comparing the measured angle α with the culculated angle α' in Table 10, it is found that α and α' are generally in accordance with each other except in some particular specimens. In hard steel, α is in good accordance with α' when the combined stresses are in phase, but it is somewhat smaller than α' when the combined stresses are not in phase. In mild steel, α is considerably smaller than α' when the applied stress is large, but it becomes nearly equal to α' when the applied stress

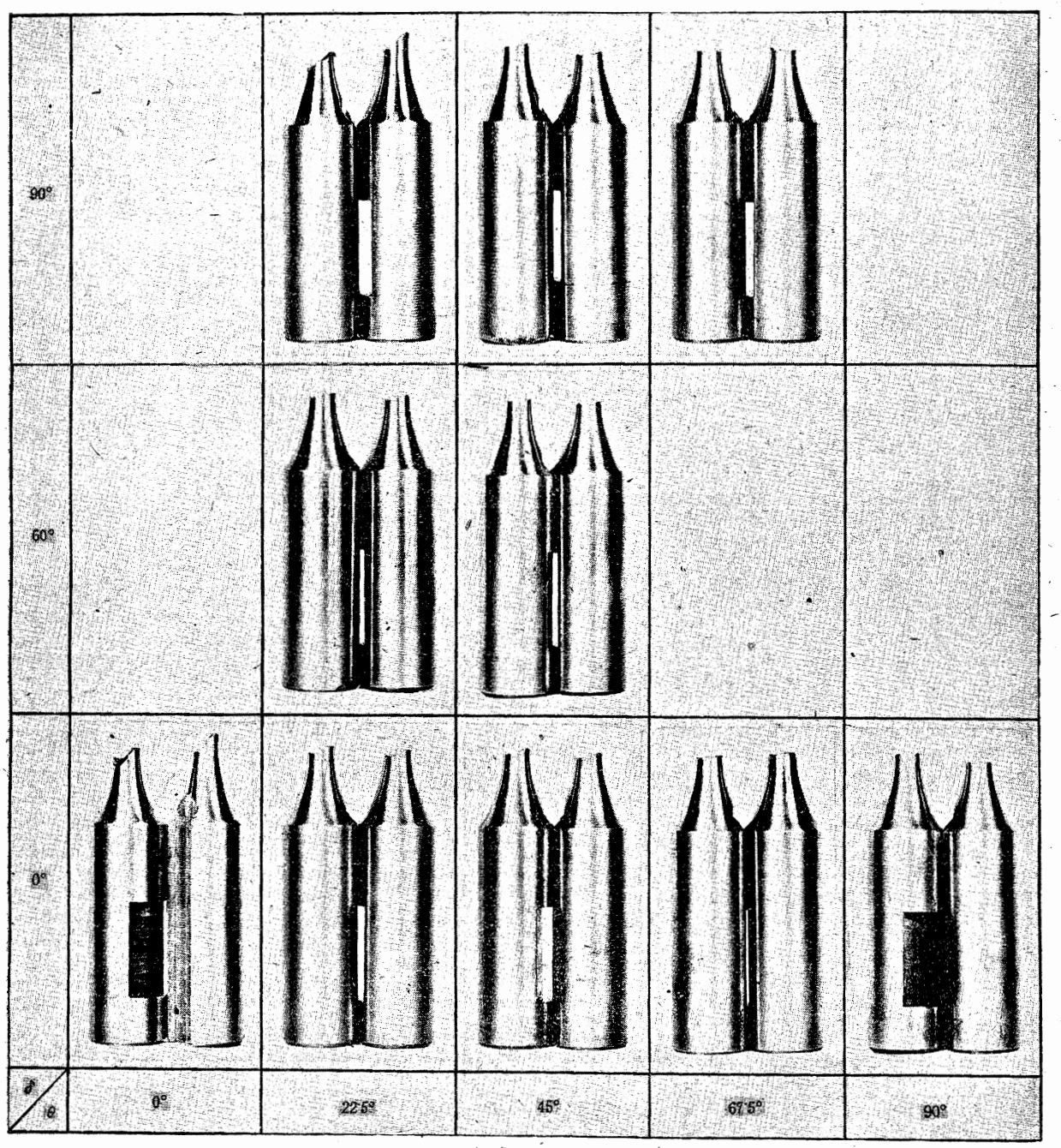

Fig. 21.

Fatigue Fractures of Mild Steel.

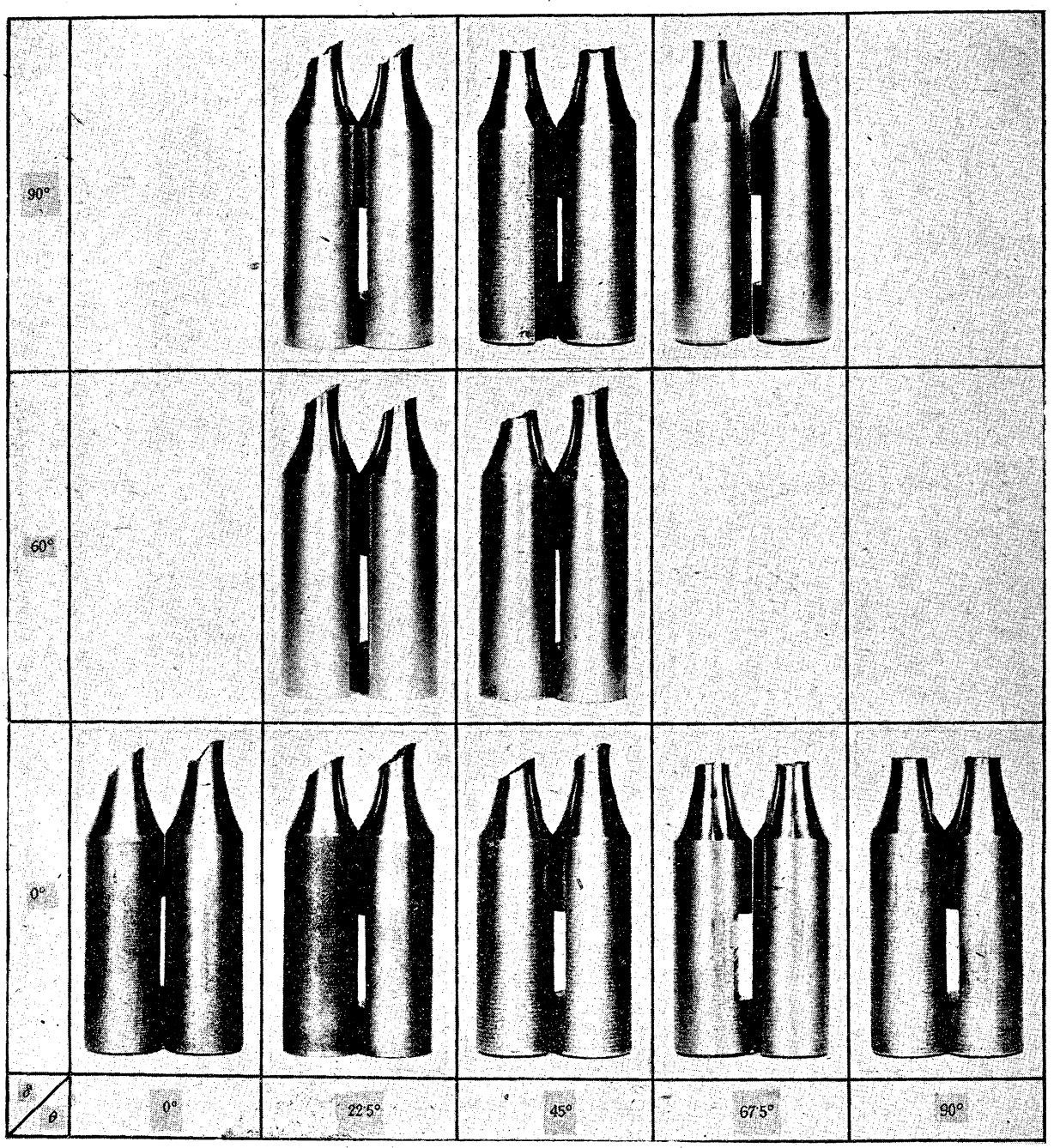

Fig. 22.
Fatigue Fractures of Cast Iron.

becomes small. This is a general characteristic in carbon steel as mentioned in the previous report. In cast iron, α is in good accordance with α' for all the specimens.

Figs. 20, 21, and 22 show the photographs of broken specimens of hard steel, mild steel, and cast iron, respectively[8]. The specimens shown in these figures are those noted with the mark (*) in Table 10.

Thus the fracture plane is approximately consistent with the plane of the greatest maximu principal stress when the combined stresses are i in phase. So we can say that the fatigue fractu of carbon steel and cast iron is always caused the maximum principal stress due to combin stresses no matter whether the stresses are in pha or not.

(2) *Fractures of duralumin.*

Fractures of duralumin are quite different fr

(8) In the photographs of broken specimens in this paper, the axis of bending moment is always in the plane of paper.

those of steels and cast iron. The angles of inclination of the fracture plane α were measured for broken specimens of duralumin and are summarized in Table 11.

Table 11.

Inclination of Fracture Plane of Duralumin to Cross Section of Specimen at point of maximum stress.

θ deg.	δ deg.	Test Piece No.	Measured Angle α, deg.	Inclination of Plane of Maximum Shear Stress to Cross Section α'', deg.
0	—	D—30 5	0	0
		„ 4	„ (*)	
		„ 3	„	
		„ 2	„	
22.5	0	„ 20	2(*)	11.25
	90	„ 24	0(*)	0
45	0	„ 12	29	22.5
		„ 11	28(*)	
		„ 16	35	
	60	„ 21	5(*)	22.5
	90	„ 15	2	Indeterminate
		„ 19	0(*)	
67.5	0	„ 22	35(*)	33.75
		„ 17	37	
	90	„ 23	32(*)	45
		„ 8	28	
90	—	„ 7	12	45
		„ 10	12	
		„ 9	15(*)	
		„ 6	14	

It has been already made clear in the previous experiments that fatigue fracture of duralumin occurs always in the direction of the maximum shear stress due to combined stresses in phase except in some specimens in pure bending. We can suppose that the fracture plane of duralumin should be consistent with the plane of the greatest maximum shear stress when the combined stresses are not in phase. The angle of inclination α'' of the plane of the greatest maximum shear stress to the cross section of the specimen is calculated and given also in Table 11. It is found that the angle α'' decreases to 0 degree from 11.25 degrees as the phase difference increases when $\theta=22.5$ degrees, while it increases to 45 degrees from 33.75 degrees when $\theta=67.5$ degrees. When $\theta=45$ degrees, it becomes constant, i. e. 22.5 degrees, independently of the applied phase difference. But when $\theta=45$ degrees and $\delta=90$ degrees, it becomes indeterminate because the maximum shear stress due to combined stresses becomes constant at every instant.

Comparing the measured angle α with the calculated angle α'' in Table 11, it is found that α is roughly in accordance with α'' except in the case of pure bending when the stresses are in phase. The result is similar as in duralumin D-24 in the previous experiments. But when the phase difference is applied to combined stresses, α becomes considerably smaller than α''. Therefore we cannot say that the fatigue fracture of duralumin is always caused by the greatest maximum shear stress due to combined stresses when the stresses are not in phase. Generally speaking, it can be recognized that in duralumin the fracture has the inclination in the direction of the greatest maximum shear stress. Here it must be noted that the number of repetitions applied to the specimens in this case is not greater than 10^7 which seems to be insufficient for the material such as duralumin.

Fig. 23 shows the photographs of the same broken specimens of duralumin which are noted with the mark (*) in Table 11.

VII. Summary.

(1) The authors have devised a new fatigue testing machine which is capable of being applied to experiments under combined bending and torsional stresses with an arbitrary phase difference. The new machine is constructed and used satisfactorily in operation.

(2) Experiments have been made with the new testing machine on four kinds of metals : hard steel, mild steel, cast iron, and duralumin. From the test results the effect of phase difference on the strength of those metals under combined alternating bending and torsion has been made clear experimentally. The fatigue limit generally increases as the applied phase difference increases. The rate of its increase due to the phase difference is greatest in cast iron and smallest in duralumin.

(3) Comparing the test results with the criterion previously proposed by the authors, it has been proved to be very satisfactory in application to test results even when the stresses are not in phase. The value of β in it seems to be independent of phase difference for carbon steels.

(4) The fracture plane of carbon steel and cast iron is nearly consistent with the plane of the greatest maximum principal stress due to combined stresses no matter whether the stresses are in phase or not.

VIII. Appendix.

All the results of experiments can be represented very well by the authors' criterion. However, as can be seen in Fig. 14, when direct and

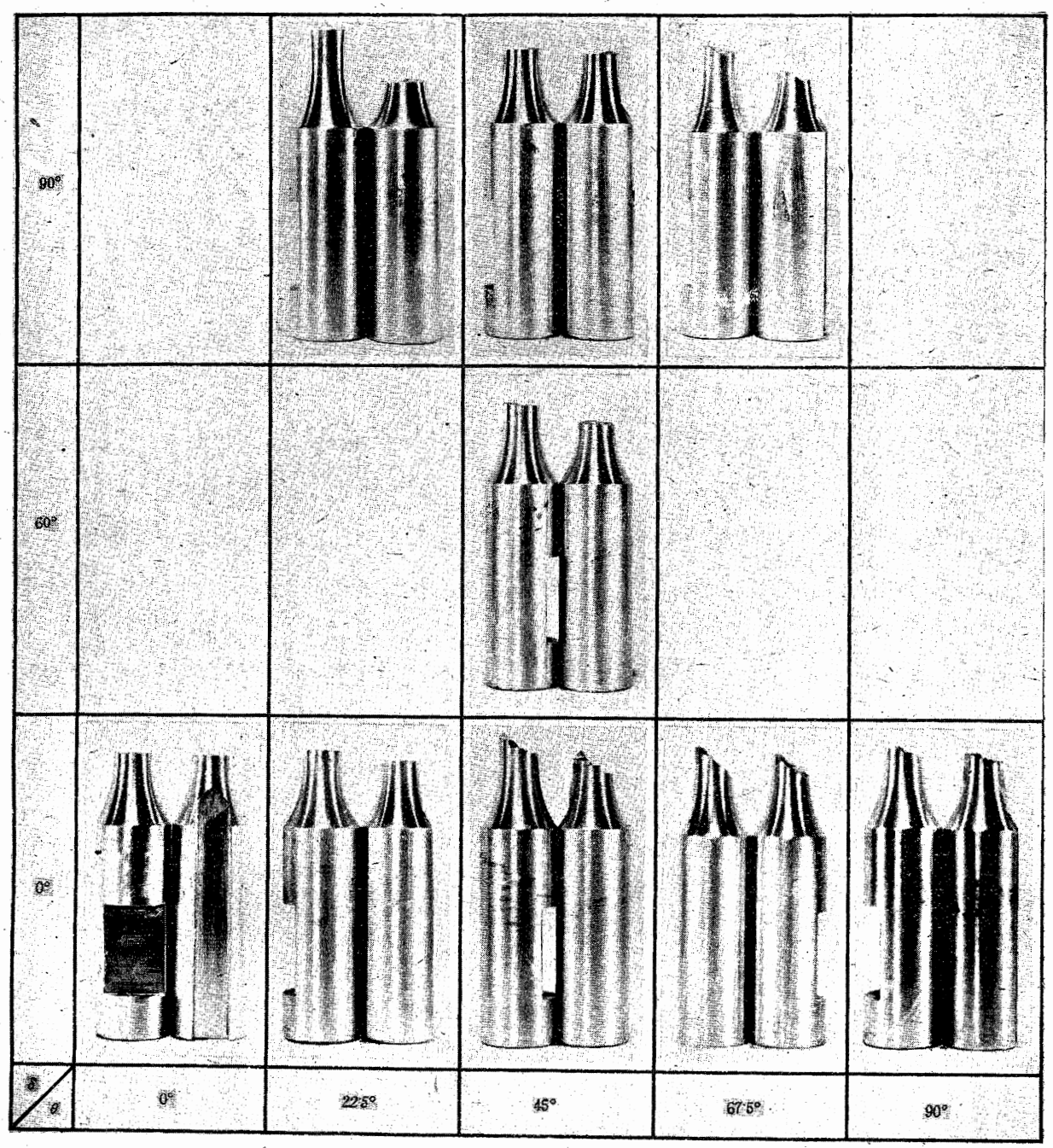

Fig. 23.

Fatigue Fractures of Duralumin.

shear stresses are in phase, the results of experiments for hard steel and duralumin are approximately in accord with the criterion of constant total strain energy, and those for mild steel and cast iron are approximately so with criterions of constant shear strain energy and constant maximum principal stress respectively.

For reference's sake, let us consider theoretically the effect of phase difference according to the following five criterions: i. e., criterions of constant maximum shear stress, of constant shear strain energy, of constant total strain energy, of constant maximum principal stress, and of constant maximu principal strain.

(1) *Criterion of constant maximum shear stre*

Applying this criterion to the case of fatigu it is considered that fatigue failure occurs when tl greatest value of the maximum shear stress induc by combined repeated stresses reaches a defini value. Then from equation (7)

$$[\sigma_a^2 \cos^2 \omega t + 4\tau_a^2 \cos^2 (\omega t - \delta)]_{\max} = \text{definite}$$

$$= \sigma_w^2 \text{ or } 4\tau_w^2 \quad (2$$

Time t in this equation must be determined when the value of the inside of the brackets becomes maximum. Putting the expression obtained by differentiating the inside of the brackets in equation (21) equal to zero, we obtain the following relation:

$$\sigma_a^2 \sin \omega t \cos \omega t + 4\tau_a^2 \sin(\omega t - \delta) \cos (\omega t - \delta) = 0 \quad (22)$$

Now let the time, when the inside of the brackets becomes maximum, be as follows:

$$t = i\frac{\delta}{\omega} \quad (23)$$

Substituting for t the value from equation (23), equation (21) and (22) become as follows:

$$\sigma_a^2 \cos^2 i\delta + 4\tau_a^2 \cos^2 (1-i)\delta = \sigma_w^2 \quad (24)$$

$$\sigma_a^2 \sin i\delta \cos i\delta - 4\tau_a^2 \sin (1-i)\delta \cos (1-i)\delta = 0 \quad (25)$$

Considering i as a parameter, we can calculate values of σ_a and τ_a for an arbitrary value of δ. Fig. 24 shows the results of calculation in a diagram. As seen in this diagram, the curve representing the relation between σ_a and τ_a is an ellipse

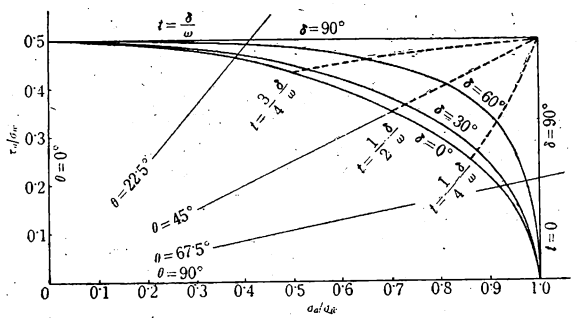

Fig. 24.

Effect of Phase Difference due to Criterion of Constant Maximum Shear Stress.

when $\delta = 0$ degree. And this curve gradually swells out as the value of δ increases. When $\delta = 90$ degrees. the curve becomes two straight lines, horizontal and vertical. That is, when $\delta = 90$ degrees and, besides, $\sigma_a > 2\tau_a$, the maximum shear stress induced by combined stresses takes the greatest value at the instant when the direct stress due to bending becomes maximum. Therefore the fatigue limit is equal to σ_w and independent of the shear stress applied. When $\delta = 90$ degrees and $\sigma_a < 2\tau_a$, the maximum shear stress induced by combined stresses takes the greatest value at the instant when the shear stress due to torsion becomes maximum. Therefore the fatigue limit is equal to $\frac{1}{2}\sigma_w$ or τ_w. and independent of the direct stress applied. The curves drawn with broken line in Fig. 24 represent the time when the maximum shear stress takes the greatest value. When $\delta = 90$ degrees and, besides, $\sigma_a = 2\tau_a$, the maximum shear stress is constant and takes the greatest value at every instant.

(2) *Criterion of constant shear strain energy.*

According to this criterion, it is considered that fatigue failure occurs when the maximum value of shear strain energy induced by combined repeated stresses reaches a definite value. Then

$$[\sigma_a^2 \cos^2 \omega t + 3\tau_a^2 \cos^2 (\omega t - \delta)]_{\max} = \text{definite} = \sigma_w^2 \text{ or } 3\tau_w^2 \quad (26)$$

Equation (26) differs from equation (21) only in the point that the coefficient of the second term in the brackets of equation (26) is 3 instead of 4 in equation (21). Therefore we can calculate values of σ_a and τ_a in the similar manner as in the preceding case. The results of calculation are shown in Fig. 25, where the relations shown are quite analogous to those in Fig. 24.

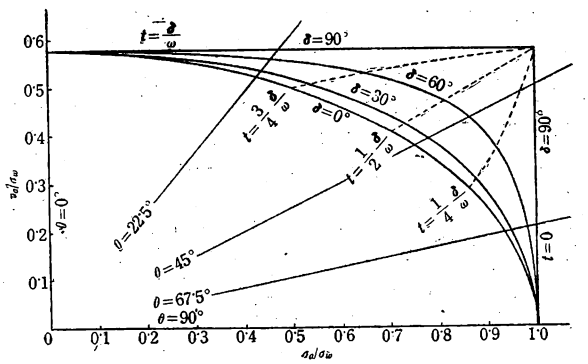

Fig. 25.

Effect of Phase Difference due to Criterion of Constant Shear Strain Energy.

(3) *Criterion of constant total strain energy.*

According to this criterion, it is considered that fatigue failure occurs when the maximum value of total strain energy induced by combined repeated stresses reaches a definite value. Then putting Poisson's constant as 10/3, the condition of fatigue failure is given with the equation

$$[\sigma_a^2 \cos^2 \omega t + 2.6\,\tau_a^2 \cos^2 (\omega t - \delta)]_{\max} = \text{definite} = \sigma_w^2 \text{ or } 2.6\tau_w^2 \quad (27)$$

Equation (27) is analogous to equation (21) or (26), therefore we can calculate values of σ_a and τ_a in the similar manner as in the preceding cases. The results of calculation are shown in Fig. 26, where the relations shown are quite analogous to those in Figs. 24 and 25.

(4) *Criterion of constant maximum principal stress.*

According to this criterion, the condition of fatigue failure is given by equation (6) as foliows:

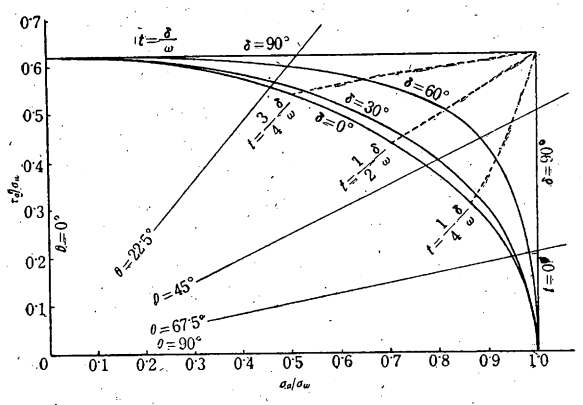

Fig. 26.

Effect of Phase Difference due to Criterion of Constant Total Strain Energy.

$$\left[\frac{1}{2}\sigma_a\cos\omega t+\frac{1}{2}\sqrt{\sigma_a^2\cos^2\omega t+4\tau_a^2\cos^2(\omega t-\delta)}\right]_{\max}$$
$$=\text{definite}=\sigma_w \text{ or } \tau_w \quad (28)$$

Putting the expression obtained by differentiating the inside of the brackets in equation (28) equal to zero, we obtain the following relation:

$$\sigma_a\sin\omega t\sqrt{\sigma_a^2\cos^2\omega t+4\tau_a^2\cos^2(\omega t-\delta)}$$
$$+\sigma_a^2\sin\omega t\cos\omega t+4\tau_a^2\sin(\omega t-\delta)\cos(\omega t-\delta)$$
$$=0 \quad (29)$$

Substituting for t the value from equation (23), equations (28) and (29) become as follows:

$$\frac{1}{2}\sigma_a\cos i\delta+\frac{1}{2}$$
$$\sqrt{\sigma_a^2\cos^2 i\delta+4\tau_a^2\cos^2(1-i)\delta}=\sigma_w \quad (30)$$

$$\sigma_a\sin i\delta\sqrt{\sigma_a^2\cos^2 i\delta+4\tau_a^2\cos^2(1-i)\delta}$$
$$+\sigma_a^2\sin i\delta\cos i\delta-4\tau_a^2\sin(1-i)\delta$$
$$\cos(1-i)\delta=0 \quad (31)$$

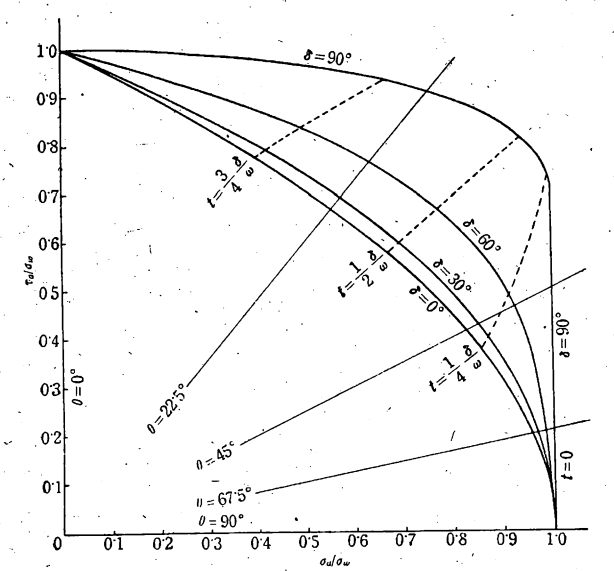

Fig. 27.

Effect of Phase Difference due to Criterion of Constant Maximum Principal Stress.

Considering i as a parameter, we can calculate values of σ_a and τ_a for an arbitrary value of δ. Fig. 27 shows the results of calculation in a diagram. The curve is a parabola when $\delta=0$ degree, and it gradually swells out as the value of δ increases. When $\delta=90$ degrees and, besides, $\sigma_a > \sqrt{2\tau_a}$, the curve becomes a vertical straight line, because the maximum principal stress induced by combined stresses takes the greatest value at the instant when the direct stress due to bending becomes maximum.

(5) *Criterion of constant maximum principal strain.*

Putting Poisson's constant as 10/3 in this criterion, the condition of fatigue failure is given by the equation

$$[0.35\,\sigma_w\cos\omega t+0.65$$
$$\sqrt{\sigma_a^2\cos^2\omega t+4\tau_a^2\cos^2(\omega t-\delta)}]_{\max}=\text{definite}$$
$$=\sigma_w \text{ or } 1.3\tau_w \quad (32)$$

Equation (32) is analogous to equation (28) and the equations differ only in values of coefficients. Therefore we can calculate values of σ_a and τ_a in the similar manner as in the criterion of constant maximum principal stress. The results of calculation are shown in Fig. 28. The relations shown in it are quite analogous to those in Fig. 27. In

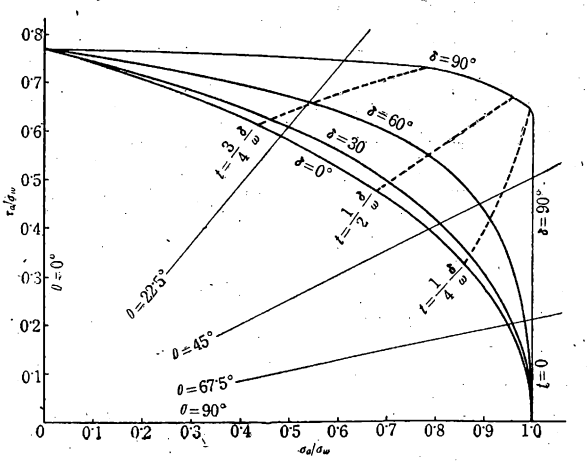

Fig. 28.

Effect of Phase Difference due to Criterion of Constant Maximum Principal Strain.

this case the relation between σ_a and τ_a is represented by a vertical straight line, when $\delta=90$ degrees and, besides, $\sigma_a > 1.61\,\tau_a$.

In the above, the effect due to phase difference according to each criterion has been made clear theoretically by calculation. Comparing these results of calculation with the results of the present experiments, it is ascertained that the fatigue limit due to those criterions is far greater than that due to experiments except the special case for cast iron.

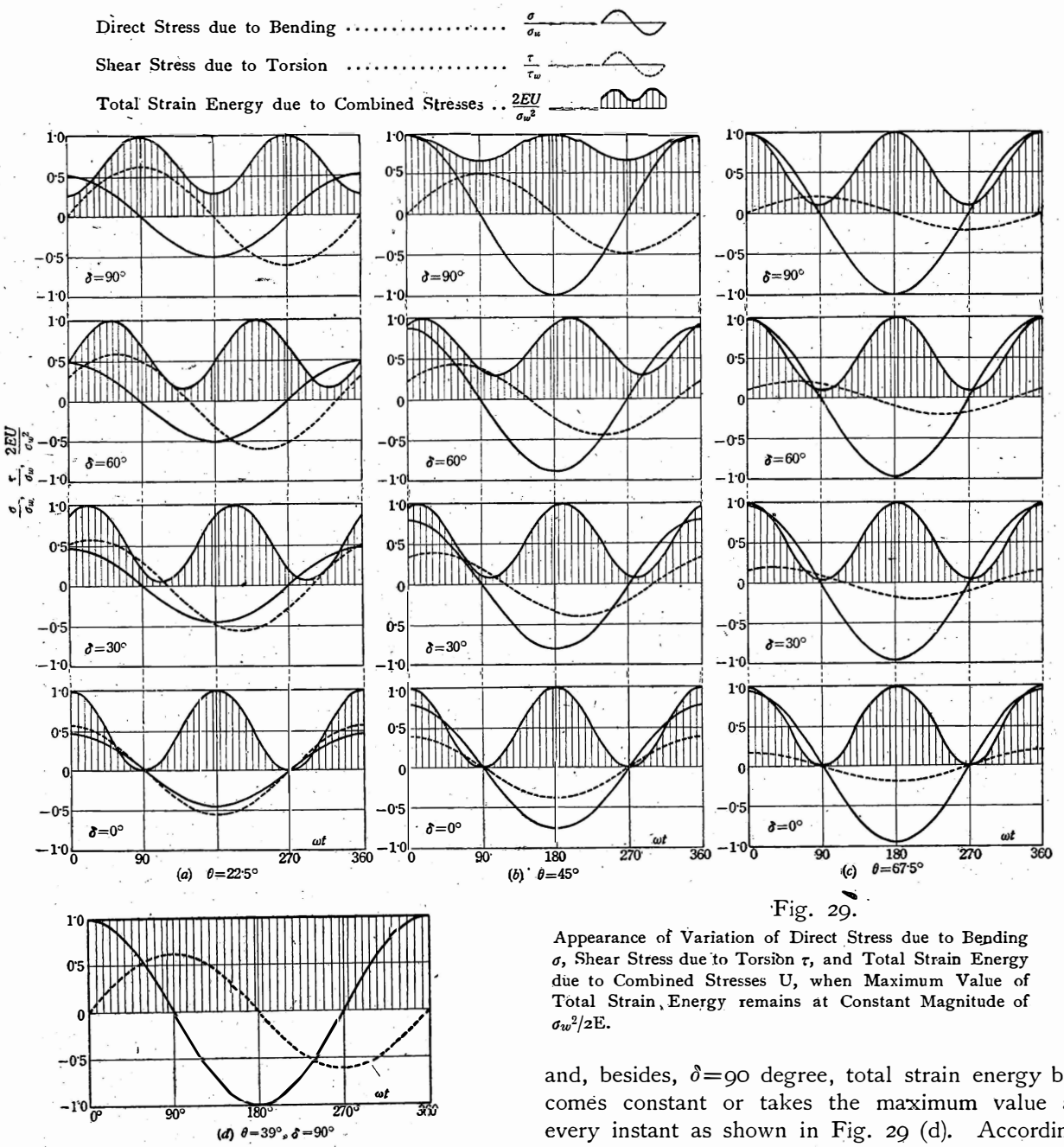

Fig. 29.

Appearance of Variation of Direct Stress due to Bending σ, Shear Stress due to Torsion τ, and Total Strain Energy due to Combined Stresses U, when Maximum Value of Total Strain Energy remains at Constant Magnitude of $\sigma_w^2/2E$.

The reason can be explained by the following consideration.

Let us, for example, consider the case of the criterion of constant total strain energy. Fig. 29 shows the appearance of variation of direct stress due to bending σ, shear stress due to torsion τ, and total strain energy due to combined stresses U during one stress period, when the maximum value of total strain energy is kept at a constant magnitude of $\frac{1}{2E}\sigma_w^2$, (where E is modulus of elasticity). As can be seen in Fig. 29 (a), (b) and (c), the minimum value of total strain energy during one period becomes larger, as the phase difference δ increases. As an extreme case when $\theta=39$ degrees and, besides, $\delta=90$ degree, total strain energy becomes constant or takes the maximum value at every instant as shown in Fig. 29 (d). According to the criterion of constant total strain energy, the material has the same resistance for fatigue in all the cases under the stress conditions shown in Fig. 29, because the maximum values of total strain energy in those cases are of the same magnitude. But examining the appearance of variation of total strain energy in Fig. 29, the reason is easily understood why the material is not so resistant to fatigue as can be estimated from the criterion when phase difference exists.

Thus it is not correct to consider that the maximum value of total strain energy is the only factor which causes the occurrence of fatigue failure, because the appearances of variation of total strain energy in those cases are very different from one another. In the opinion of the authors it is reason-

able to regard that the sum of the maximum total strain energy due to bending and that due to torsion exerts also an influence upon the occurrence of the fatigue failure. As mentioned in the previous report, the authors' criterion for the case with phase difference has been derived on the basis of this idea.

The cost of this research has been defrayed from the Scientific Research Appropriation of the Department of Education.